

NWP SAF

Satellite Application Facility for Numerical Weather Prediction

Document NWPSAF-MO-VS-034

Version 1.0

13 December 2007

Investigation of the suitability of the 6S radiative transfer model to extend RTTOV to solar wavelengths

Nicolas Huneeus

Laboratoire d' Optique Atmospherique



Investigation of the suitability of the 6S radiative transfer model to extend RTTOV to solar wavelengths

Nicolas Huneeus

Laboratoire d'Optique Atmosphérique

*Universite des Sciences et Techniques de Lille u.e.r. de Physique Fondamentale,
59655 Villeneuve d'Ascq Cedex, France*

This documentation was developed within the context of the EUMETSAT Satellite Application Facility on Numerical Weather Prediction (NWP SAF), under the Cooperation Agreement dated 1 December, 2006, between EUMETSAT and the Met Office, UK, by one or more partners within the NWP SAF. The partners in the NWP SAF are the Met Office, ECMWF, KNMI and Météo France.

Copyright 2007, EUMETSAT, All Rights Reserved.

| Change record | | | |
|---------------|----------|---------------------|---------------------|
| Version | Date | Author / changed by | Remarks |
| 0.1 | 26.11.07 | N. Huneeus | Initial draft |
| 1.0 | 13.12.07 | N. Huneeus | Version for release |
| | | | |
| | | | |
| | | | |
| | | | |



Investigation of the suitability of the 6S radiative transfer model to extend RTTOV to solar wavelengths

Nicolas Huneus

Laboratoire d'Optique Atmosphérique

*Université des Sciences et Techniques de Lille u.e.r. de Physique Fondamentale, 59655 Villeneuve d'Ascq
Cedex,
France*

Under guidance from:

Didier Tanré (CNRS, LOA)

Olivier Boucher (Met Office)

NWP SAF contact:

Roger Saunders (Met Office)

Table of contents

| | |
|--|-----------|
| TABLE OF CONTENTS | 3 |
| 1 INTRODUCTION..... | 4 |
| 2 ORIGINAL 6S AND ITS ADAPTED VERSION | 4 |
| 2.1 6S: A SHORT DESCRIPTION..... | 4 |
| 2.2 MODIFICATIONS INTRODUCED INTO 6S | 4 |
| 3 VALIDATION OF 6S GEMS | 6 |
| 3.1 ACCURACY | 6 |
| 3.2 PORTABILITY AND EXECUTION TIME | 7 |
| 4 CONCLUSIONS AND RECOMMENDATIONS..... | 9 |
| 4.1 SUMMARY..... | 9 |
| 4.2 RECOMMENDATIONS | 9 |
| 5 REFERENCES..... | 9 |
| 6 APPENDIX A: DESCRIPTION OF ROUTINES IN 6S-GEMS..... | 10 |
| 7 APPENDIX B: VALIDATION FIGURES | 13 |

Introduction

The NWP SAF is considering extending its radiative transfer model RTTOV (from **R**adiative **T**ransfer for **T**OVS) into the solar spectrum. There is also some interest in a fast model for calculating radiances in the solar spectrum within the “Global and regional Earth-system (Atmosphere) Monitoring using Satellite and in-situ data (GEMS)” project. We explore the suitability of using the “Second Simulation of the Satellite Signal in the Solar Spectrum” radiative transfer model (hereafter 6S) for this purpose (Vermote et al., 1997a and Vermote et al., 1997b). This report presents the modifications introduced into 6S to fit the GEMS project requirements and to follow stricter coding standards, such as those used at ECMWF or for RTTOV. Section 2 describes briefly the original 6S model and presents the modifications introduced into the model. In section 3 the results of the validation of the adapted version of 6S are presented. Since most of this work in adapting 6S was done in the framework of the GEMS project, we keep the name of 6S-GEMS initially given to the modified version. Finally, the conclusions of this work and some recommendations are given in Section 4.

Original 6S and its adapted version

6S: a short description

The model simulates the solar radiation reflected by the surface-atmosphere system as measured by satellite. These calculations are done for a wide range of conditions; the reflectance can be calculated for a given wavelength or for predefined spectral bands of existing satellite measurements. It can also calculate the reflectance starting from the total optical thickness at 550 nm or the equivalent visibility expressed in km. Many options are also available to define the aerosol models. The user can either choose standard aerosol models or define a model by setting the percentage among 4 available aerosol components or define the model through a size distribution function or solar photometer measurements. Finally, the aerosol model can also be given as input to the model. These features make 6S a flexible tool capable for simulating multiple measurement scenarios.

The reflectance measured by the satellite, or apparent reflectance, for a Lambertian and homogeneous surface is calculated considering the contribution of the intrinsic reflectance of the atmosphere and the total solar radiation (direct and diffuse) reflected by the surface and directly transmitted to the instrument. The atmospheric reflectance takes into account the surface reflection, molecular and aerosol scattering, and the coupling between them. The molecular scattering is estimated considering a standard atmosphere with molecules distributed vertically with an exponential density with 8 km scale height whereas the aerosol component is calculated assuming a scale height of 2 km with constant vertical optical properties. The computations are done using the method of successive order of scattering (Deuzé et al., 1989). This method computes the total atmospheric reflectance by calculating the contribution of each additional interaction of solar radiation with spherical particles.

Modifications introduced into 6S

The modifications introduced to 6S can be separated into two groups; those that adapt the radiative transfer code to the inputs and outputs of an atmospheric NWP model (and to a large extent to RTTOV) and those that update the language from fortran77 to fortran90 in order to fit stricter coding standards and try to make it computationally more efficient. This last group of changes considers for instance the replacements or deletion of *GOTO* instructions, the inclusion of *WHILE* statements instead of some *IF* statements, the suppression of all *COMMON* as a means of data exchange between subroutines and the reordering of the subroutines in order to avoid making unnecessary calculations.

The first group of changes eliminates some of the flexibility of the model and adapts it to a given set of input variables. While 6S is a flexible model capable of simulating multiple measurement scenarios, 6S-GEMS was conceived in order to calculate the radiance for a set of wavelengths and as a function of the vertical distribution of aerosol optical depth and properties which are now given as input variables. These last two features, vertical profile of optical properties and optical depth given as input, are responsible for most of the transformations in 6S-GEMS. In order to better present the modifications introduced, a short description of the model will follow. The schematic representation of 6S-GEMS is shown in Figure 1, each subroutine with a list of its inputs and outputs is presented in Appendix A while the code of each subroutine is given in Appendix B.

The radiative transfer model 6S delivers the reflectance for a single grid point at a time whereas 6S-GEMS does it for an array of grid points. In order to implement this, the core radiative transfer calculations were embedded into two consecutive loops, a first one on the grid points and a second one on the wavelength. This construction was chosen, rather than having the loops inside each subroutine, in order to facilitate the parallelization of the code. Since the reflectance computations for each grid point can be considered independent from its neighbours, the chosen structure allows splitting the grid point array in several domains and making the computation for each domain independently (domain decomposition).

Calculations independent of intermediate results are done prior to the loops containing the core calculations. This is done to reduce the computing time and thus optimize the code. This applies to the computation of the Gaussian angles and weights, the components of the Legendre polynoms of the phase function for each element of the Fourier series and the discretization of aerosol vertical variables. The user provides 6S-GEMS with a profile of optical depth and the corresponding phase function and single scattering albedo for each layer. This input optical depth profile has a vertical distribution according to the discretization of the transport model providing this information. However this allows individual model layers to have high aerosol load which can lead to errors in the reflectance. In order to minimize this error, the original vertical distribution is converted into one with layers of constant optical thickness. This ensures that the model will have a large number of thin layers at levels with large aerosol concentrations. The total number of layers in the radiative transfer model does not have to be the same as in the host atmospheric model. However the execution time of 6S-GEMS is sensitive to this parameter and therefore a sensitivity study for the appropriate number of layers is recommended to be conducted prior to each application of the model.

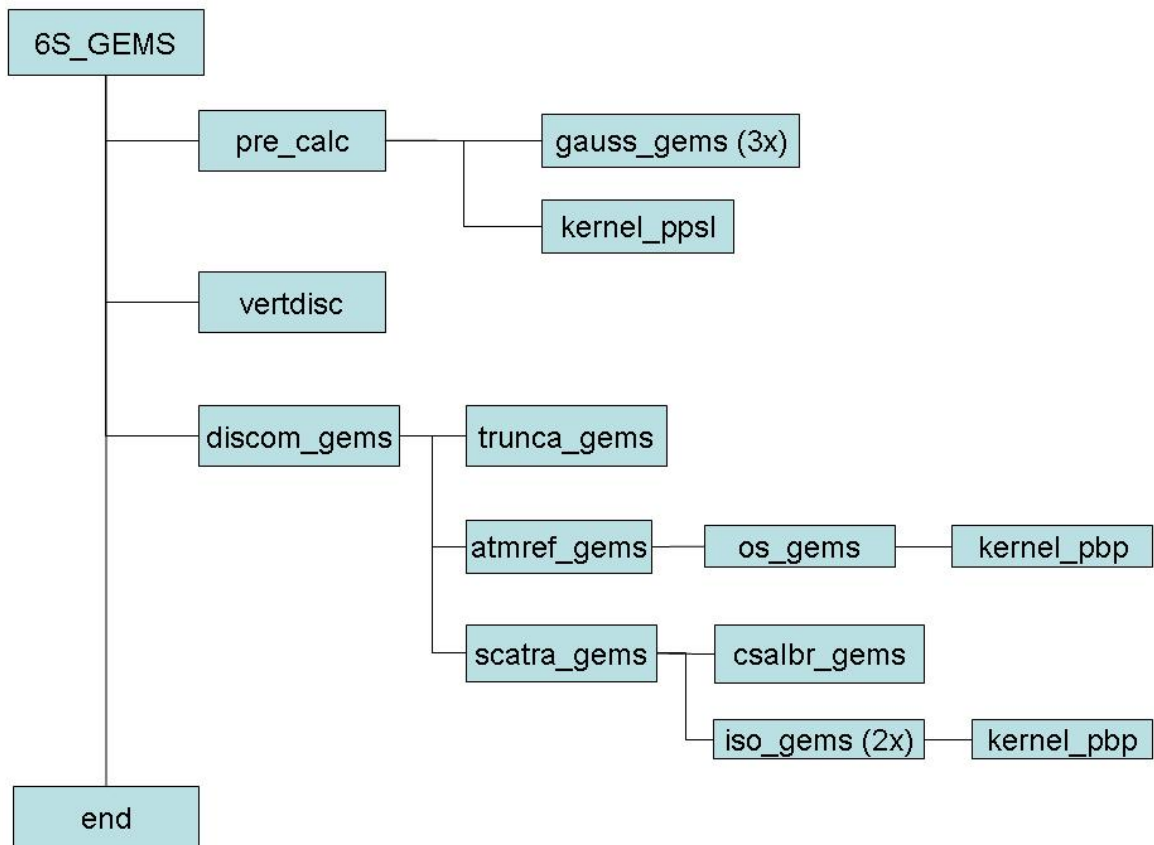


Figure 1: Flowchart of 6S-GEMS. Subroutines with suffix gems are based on subroutines from the original 6S model named as the prefix.

| 6S | 6S-GEMS |
|--|--|
| Fixed vertical profile | Variable vertical profile |
| Fixed aerosol model on the vertical | Variable aerosol model on the vertical |
| Integration over satellite wavebands | Calculation at single wavelength |
| Calculations of reflectances for aerosols, molecules and mixture | Calculation of reflectances only for the molecules-aerosols mixture |
| Specular reflection accounted for | No specular reflection (results valid only outside the glitter region) |

| | |
|---|---|
| Different representations of surface reflectance | Assumption of a homogeneous surface |
| Flexible inputs | Inputs are AOD, single scattering albedo and phase function at each layer |
| Flexibility to simulate different types of measurements | Simulates only satellite measurements |
| Gaseous absorption | No gaseous absorption |

Table 1: Summary of differences between 6S and 6S-GEMS

The core radiative transfer subroutines are taken from the original model and modifications were introduced to update the language and format, optimize the efficiency of the code and introduce the necessary changes in order to allow the vertical variability of optical properties in the calculations. Besides the above-mentioned modifications, some additional features contained in 6S were also eliminated. We neglect the impact of the specular reflection (or glitter) of the ocean surface on the final signal. We consider the target reflectance to be independent from the environment which is equivalent to assuming a homogeneous surface. We eliminated the effect of the gaseous absorption in the reflectance. This error can be minimized by the appropriate choice of wavelengths. Finally, we also neglected the polarization of light due to aerosols, a feature available in the latest version of 6S.

Validation of 6S GEMS

The goal from the present validation is twofold, namely to examine the model's performance in term of its accuracy to reproduce the 6S's radiances and its execution time and portability. This last is due to its potential application in RTTOV.

Accuracy

In order to validate 6S GEMS we will compare its results in terms of radiance with the ones calculated by 6S, we will also include the results obtained from a third radiative transfer model known as successive order or OS (Deuzé et al., 1989). This model computes the multiple interactions of spherical particles with solar radiation by evaluating the contribution of each additional scattering interaction to the total atmospheric reflectance. It takes into account not only the specular reflection of the ocean surface but also de polarization due to aerosols. OS is expected to be a more accurate radiative transfer model than 6S, especially at shorter wavelengths where polarisation of light has a more important role. The reflectance calculations of 6S, and therefore also of 6S GEMS, are based on this model but without polarisation. Due to the above, we consider the results from OS as the "truth" for the present validation. The radiance calculated by OS, but neglecting polarization of light and specular reflection (OS NOPOL), will also be included in the validation in order to present the differences it introduces in the results. We will present the radiance of each one of the models for varying optical thickness that span the range from 0.075 to 1.5 and for a given set of viewing geometries. The computations will be conducted considering four fine modes and one coarse mode (Table 2). The calculations will be repeated for wavelengths of 565, 670 and 865 nm and for real part of refractive index of 1.35, 1.45 and 1.60 for fine mode and refractive index of 1.33, 1.35 and 1.37 for coarse mode aerosols. For all the cases no aerosol absorption will be considered (imaginary part of refractive index equal to zero).

| | Model | Radius [μm] | Standard deviation |
|--------------------|-------|--------------------------|--------------------|
| Fine mode | 1 | 0,04 | 0,46 |
| | 2 | 0,08 | 0,46 |
| | 3 | 0,1 | 0,46 |
| | 4 | 0,13 | 0,46 |
| Coarse mode | 1 | 0,75 | 0,7 |

Table 2: Aerosol size distribution of fine and coarse modes as used in the validation of 6S GEMS.

For practical reasons we will discuss the validation of 6S GEMS considering only one particular case among the ones calculated. The remaining cases will be presented in Appendix C. The chosen configuration presented one of the largest differences with 6S and OS in the initial inspections of the performance of the model. We will consider the radiance for a wavelength of 865 nm, fine mode model N°1 and real part of refractive index of 1.35. The calculations were repeated for the coarse mode model.

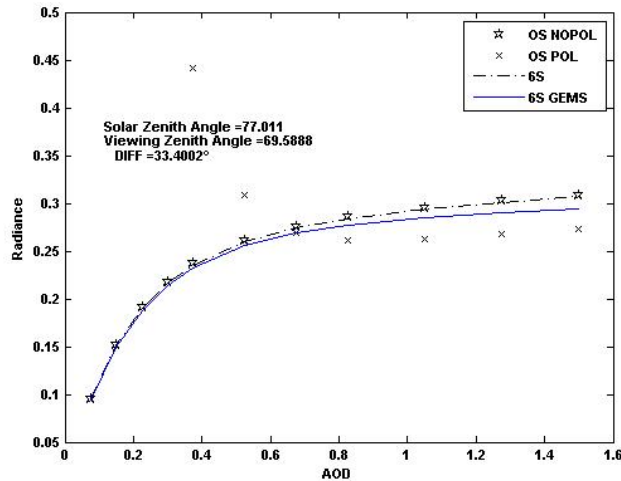


Figure 2: Radiances according to 6S (black discontinuous), 6S GEMS (blue), OS (stars) and OS without polarization and glitter (black cross). The results correspond to a wavelength of 865 nm, a difference in azimuthal angle of 180° and a refractive index of 1.35. a) Fine mode with mean modal radius of $0.04 \mu\text{m}$, standard deviation of 0.46.

For the case of fine aerosols, the three models OS NOPOL, 6S and 6S GEMS underestimate the radiance of OS (when polarization and specular reflection are considered) up to an optical thickness of 0.675 after which they overestimate the radiance. However when the effect of polarization and glitter is removed, 6S reproduces the radiances of OS NOPOL for all optical thickness. 6S GEMS reproduces closely the radiances of 6S but presents differences that increase with increasing optical thickness. The maximum difference between these models is of approximately 4% for an optical thickness of 1.5 (Figure 2). In the case of coarse particles, the three models (OS NOPOL, 6S and 6S GEMS) underestimate the radiance of OS for all optical thicknesses but with a decreasing difference with increasing optical thickness. The results from 6S underestimates the radiance from OS but overestimates the radiance from OS NOPOL, whereas 6S GEMS underestimates the radiance of both 6S and OS for all optical thickness (Figure 3).

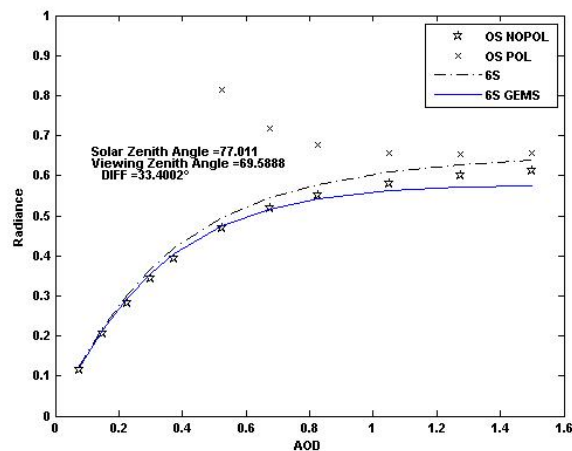


Figure 3: Same as Figure 2 but for coarse mode with mean modal radius of $0.75 \mu\text{m}$ and standard deviation of 0.69.

Portability and execution time

Since the final goal of the model is to be applied in operational forecast, not only the numerical result is important but also the execution time. Therefore we compare 6S-GEMS to the original version not only in terms of radiance but also computational time. In order to test the portability of the model, it was compiled and executed successfully on three different computers with three different architectures. It has been tested on an IBM server with a Unix environment and a xlf90 Fortran compiler (labelled LOA in Figure 4). It has also been tested on a personal computer with an Intel processor and a Linux environment with the Portland Group Fortran pgf90 (labelled Metoffice in Figure 4). Finally, it was also tested on an Intel server with Unix environment and ifort Fortran compiler (labelled LSCE in Figure 4). No particular compiling optimisation options were included. Results from these machines show the same results (within the machine precision) in terms of radiance (Figure 4) but large differences in execution time from one machine to the other (Table 2). In spite of their differences in execution time, all three of them spend most of their

time in the subroutine Kernel_pbp (for a detail of this subroutine see Appendix A). LOA and LSCE spend close to 70% of their time in it while Metoffice spends only 60% of its time.

| | LOA | LSCE | Metoffice |
|----------------------|--------------|--------------|--------------|
| Gauss_gems zenith | 0,000 | 0,000 | 0,000 |
| Gauss_gems azimuth | 0,000 | 0,000 | 0,000 |
| Gauss_gems trunca | 0,000 | 0,001 | 0,000 |
| Kernel_ppsl | 0,030 | 0,012 | 0,009 |
| Pre_calc | 0,030 | 0,013 | 0,010 |
| Vertdisc | 0,020 | 0,016 | 0,039 |
| Trunca_gems | 0,000 | 0,001 | 0,002 |
| Kernel_pbp | 0,670 | 0,921 | 0,294 |
| Os_gems mixture | 0,700 | 0,934 | 0,319 |
| Atmref_gems | 0,700 | 0,934 | 0,319 |
| Kernel_pbp | 0,100 | 0,154 | 0,068 |
| Iso_gems UT* | 0,110 | 0,156 | 0,072 |
| Kernel_pbp | 0,090 | 0,142 | 0,040 |
| Iso_gems DT** | 0,100 | 0,144 | 0,043 |
| Scatra_gems | 0,210 | 0,300 | 0,116 |
| Discom_gems | 0,910 | 1,235 | 0,437 |
| 6S-GEMS Total | 0,970 | 1,269 | 0,489 |

Table 2: Execution time (in seconds) of each subroutine and total execution time of 6S-GEMS on three different machines; Laboratoire d'Optique Atmosphérique (LOA), Laboratoire des Sciences du Climat et de l'Environnement (LSCE) and Met Office (Metoffice). UT*= upward transmission. DT**=downward transmission.

The original version of 6S takes approximately 0.47 seconds to calculate the reflectance in the IBM machine with Unix environment (LOA). The modified version however needs 0.97 seconds of CPU time to compute the reflectance from which nearly 70 % of the CPU time is spend in the kernel calculations (subroutine Kernel_pbp.f). This subroutine calculates the aerosol phase function and the components of the Legendre decomposition of the phase function. The original model considers a fixed aerosol model on the vertical and therefore requires the kernel computations only once. 6S-GEMS, however, considers a phase function with vertical variability corresponding the change of aerosol model from layer to layer. This vertical variability forces to do the kernel computations at each model layer with the consequent increase in execution time (see our recommendations on how to address this).

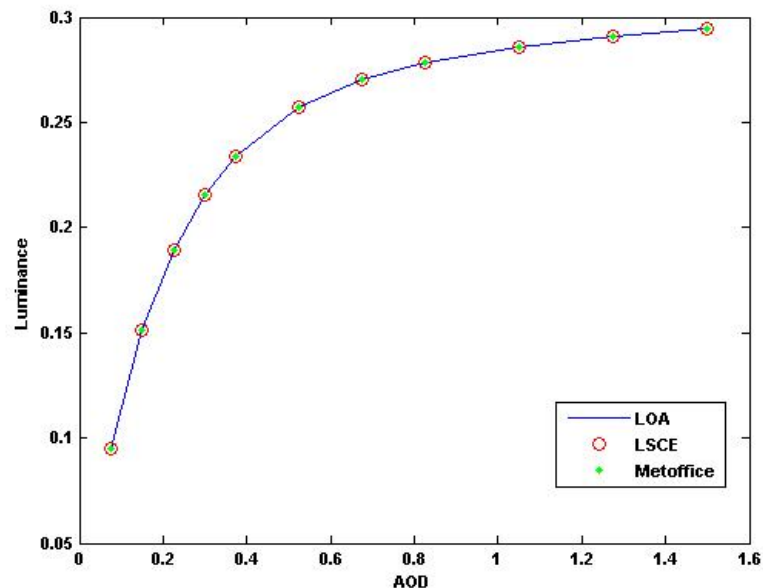


Figure 4: Radiance at 865 nm for fine mode aerosol with mean model radius of 0.04 μm , standard deviation of 0.46 and refractive index of 1.35. Results from 6S GEMS from three different environments. LOA: IBM server with a Unix environment and a xlf90 Fortran compiler, Metoffice: personal computer with an Intel processor and a linux

environment with the Portland Group Fortran pgf90, LSCE: Intel server with Unix environment and ifort Fortran compiler.

Conclusions and recommendations

Summary

The radiative transfer model 6S was adapted in order to follow stricter coding standards and fit the data flow of RTTOV. The flexibility of 6S to simulate multiple measuring scenarios was eliminated in order to simulate the radiance as measured by a satellite at a given wavelength, a mixture of aerosol models and for a vector of grid points. The main modifications introduced into 6S-GEMS are associated to the inclusion of vertical variability of the aerosol model.

The adapted 6S-GEMS model successfully reproduces the radiances for different viewing geometries, wavelength and aerosol models. It shows difficulties, both for fine aerosols as for coarse ones, only in reproducing the radiance at low optical thickness when the specular reflection of the ocean surface is important. However, these cases correspond to conditions where the inversion is usually not conducted and therefore does not influence the potential of the model to be used in the inversion or assimilation of aerosol properties.

Recommendations

The feasibility of applying 6S-GEMS in RTTOV was discussed in a meeting together with Roger Saunders (Manager SIAG, Met Office R&D) and Olivier Boucher (Hd CCE, Met Office Hadley Centre). More work has to be conducted before including 6S-GEMS in RTTOV. Some of the pending tasks include:

- Calculation of the Rayleigh optical thickness profile at 550 nm from the temperature and pressure profiles provided by RTTOV. This can be done either inside 6S-GEMS or in the interface of the two models.

In order to optimise the code further, we recommend to:

- Decouple the vertical discretisation of the vertical profile of aerosol optical depth and that of the aerosol model (the aerosol optical depth would be discretised on the full grid whereas the aerosol model could be discretised on a reduced grid. This would reduce the number of calls to the expensive kernel routines. A factor of 8 speed up in the execution time seems achievable. The impact this has on accuracy would have to be tested for typical profiles involving aerosol mixtures).
- Optimise the number of iterations in the `os_gems` (There is a balance to be achieved between accuracy and speed here. Moreover the code would benefit from a rewriting of the convergence criteria.).
- Optimise the number of terms in the decomposition of the phase function in each iteration. In this approach, the primary scattering, which represents most of the signal for the usual range of aerosol optical thickness, less than 1.0, is computed using the exact phase function. Then the multiple scatterings are computed using a limited number of terms of the phase function since the radiation is more and more isotropic as the number of scattering increases. The required number of terms can be adjusted depending on the asymmetry parameter of a given aerosol type.

References

- Deuzé, J.L., M. Herman, and R. Santer (1989), Fourier series expansion of the transfer equation in the atmosphere-ocean system, *J. Quant. Spec. Rad. Transfer*, 41(6), 483-494.
- Vermote, E., D. Tanré, J.L. Deuzé, M. Herman, and J.J. Morcrette (1997a), Second Simulation of the Satellite Signal in the Solar Spectrum: An overview, *IEEE Trans. Geosci. Remote Sens.*, 35(3), 675-686.
- Vermote, E., D. Tanré, J.L. Deuzé, M. Herman, and J.J. Morcrette (1997b), Second Simulation of the Satellite Signal in the Solar Spectrum, *6S User guide version 2*, 53 pp.

Appendix A: Description of routines in 6S-GEMS

Each routine is presented with a short description of what it does as well as a list of its inputs/outputs and their dimensions. The routines are presented in the same order as they are called (Figure 1). It will be indicated in each case if the routine is taken from the original version of 6S. In those cases further details of the routines can be found in the manual of 6S (Verote et al., 1997b).

6S GEMS: Main calling routine.

Input:

pdiffang[klon]=difference in azimuthal angle [radianes]. Viewing minus solar azimuthal angle.
 psolang[klon] = solar zenithal angle [degrees]
 pvieang[klon] = viewing zenithal angle [degrees]
 pwl[kwl] =wavelengths at which the calculations are done [m]
 ptray550_vertin[klon,0:klev] = rayleigh optical thickness profile at 0.55e-6 m
 ptaer_vertin[klon,0:klev,kwl] = aerosol optical thickness profile
 phasel_in[klon,0:klev,nwl,nbmu] = aerosol phase function profile
 piz_in[klon,0:klev,kwl] = aerosol single scattering albedo profile
 proc[klon,nwl] = target surface reflectance

Output:

reflet[klon,kwl] = apparent reflectance at kwl wavelength

PRE_CALC: Preliminary calculations for gauss integrations and successive order of scattering. This subroutine includes calculations from the original routines GAUSS.f and KERNEL.f

Input: pvieang[klon] = viewing zenithal angle [degrees]
 psolang[klon] = solar zenithal angle [degrees]

Output:

prp [knp] = Gaussian angles for the azimuth [rad]
 pgp [knp] = Gaussian weights for the azimuth
 prm [-kmu:kmu] = Gaussian angles for the zenith [in cosine]
 pgb [-kmu:kmu] = Gaussian weights for the zenith
 prmu[knbmu] = Gaussean angles for truncation of the phase function [in cosine]
 pga[knbmu]=Gaussian weights for truncation of the phase function
 ppl[knbmu,-1:knang+1]=components of the legendre polynome of the phase function.
 ppsl[klon,0:knang,-1:knang,-kmu:kmu]=components of the Legendre polynome of the phase function for each element of the Fourier series.

GAUSS GEMS: Calculations of angles and weights for gauss integration. Based on the subroutine GAUSS.f from 6S.

Input:

px1= lower angular limit
 px2 = upper angular limit
 kn = number of angles to be considered (can be either knp or kmu)

Output:

px[kn] = Gaussian angles
 pw[kn] = Gaussian weights

KERNEL PPSL: Compute the values of Legendre polynomials used in the successive order of scattering method. Based on the subroutine KERNEL.f from 6S.

Input:

prm[-kmu:kmu] = gaussean zenithal angles

Output:

ppsl[klon,0:knang,-1:knang,-kmu:kmu]=components of the Legendre polynome of the phase function for each element of the Fourier series.

VERTDISC: Changes the given vertical distribution of aerosol optical thickness into a vertical distribution with layers of constant optical thickness. It calculates the phase function and single scattering albedo corresponding to the new optical thickness profile. Starting from the molecular optical thickness profile at 550 nm given as input, the subroutine computes the rayleigh optical thickness at all *kw* wavelengths. *Klev* is number of levels at input and *knt* is the number of levels at output.

Input:

pwl[nwl] = wavelengths at which the calculations are done [m]
 ptray550_vertin[klon,0:klev] = rayleigh optical thickness profile at 0.55e-6 m
 ptaer_vertin[klon,0:klev,kwl] = aerosol optical thickness profile
 phasel_in[klon,0:klev,kwl,nbmu] = aerosol phase function profile
 piz_in[klon,0:klev,kwl] = aerosol single scattering albedo profile

Output:

ptaer_vert[klon,0:knt,kwl] = aerosol optical thickness profile
 ptray_vert[klon,0:knt,kwl] = rayleigh optical thickness profile
 phasel[klon,0:knt,kwl,nbmu] = aerosol phase function profile
 piz[klon,0:knt,kwl] = aerosol single scattering albedo profile

DISCOM_GEMS: Computes optical properties of the atmosphere at requested wavelength. Based on DISCOM.f from 6S.

Input:

phirad= difference of azimuthal angles [radians]
 pxmus= cosine of solar zenith angle
 pxmuv= cosine of viewing zenith angle
 prp[knp] = angles for the gauss integration over the azimuth [rad]
 prmu[knbmu] = Gaussean angles for truncation of the phase function [in cosine]
 pga[knbmu]=Gaussian weights for truncation of the phase function
 ppl[knbmu,-1:knang+1]=components of the legendre polynome of the phase function.
 ppsl[klon,0:knang,-1:knang,-kmu:kmu]=components of the Legendre polynome of the phase function for each element of the Fourier series.

Output:

roatm[3] = atmospheric reflectance
 dtmdir[3] = downward direct transmittance
 dtdif[3] = downward diffuse transmittance
 utmdir[3] = upward direct transmittance
 utdif[3] = upward diffuse transmittance

TRUNCA_GEMS: Truncation of the phase function and computation of the coefficients of the Legendre polynome. Based on the original subroutine TRUNCA.f of 6S

Input:

phasef[klon,nt,nwl,nbmu] = phase function
 prmu[knbmu] = Gaussean angles for truncation of the phase function [in cosine]
 pga[knbmu]=Gaussian weights for truncation of the phase function
 ppl[knbmu,-1:knang+1]=components of the legendre polynome of the phase function.

Output:

pcoeff[0:knt] = truncation coefficient
 pbetal[0:knt,0:knang] = coefficients of the Legendre polynome.
 phasef[klon,nt,nwl,nbmu] = phase function

ATMREF_GEMS: Calculates aerosol, rayleigh and mixture reflectance. Base on the original subroutine ATMREF.f of 6S.

Input:

prp[knp] = angles for the gauss integration over the azimuth [rad]
 pgb [klon,-kmu:kmu] = Gaussian weights for the zenith
 prm [-kmu:kmu] = Gaussian zenithal angles [in cosine]

phirad = difference of azimuthal angles [radians]
 pxmus = cosine of solar zenith angle
 pxmuv = cosine of viewing zenith angle
 ptamoy [0:knt] = aerosol optical thickness profile (truncated in discom.f)
 ptray[0:knt,] = rayleigh optical thickness profile
 pizmoy[0:knt] = corrected scattering albedo
 ptodaer = total aerosol optical depth
 ptodray = total molecular optical depth
 pbetal[0:knt,0:knang] = coefficients of the Legendre polynome.
 ppsl[klon,0:knang,-1:knang,-kmu:kmu]=components of the Legendre polynome of the phase function for each element of the Fourier series.

Output:

prorayl = rayleigh reflectance
 proaero = aerosol reflectance
 promix = reflectance of mixture
 prn [-kmu:kmu] = Gaussian zenithal angles [in cosine]

OS_GEMS: Computation of the atmospheric intrinsic reflectance. Based on the original subroutine OS.f of 6S.

Input:

prp[knp] = angles for the gauss integration over the azimuth [rad]
 pgb [klon,-kmu:kmu] = Gaussian weights for the zenith
 prn [-kmu:kmu] = Gaussian zenithal angles [in cosine]
 phirad = difference of azimuthal angles [radians]
 ptamoy [0:knt] = aerosol optical thickness profile (truncated in discom.f)
 ptray[0:knt,] = rayleigh optical thickness profile
 pizmoy[0:knt] = corrected scattering albedo
 ptodaer = total aerosol optical depth
 ptodray = total molecular optical depth
 pbetal[0:knt,0:knang] = coefficients of the Legendre polynome.
 ppsl[klon,0:knang,-1:knang,-kmu:kmu]=components of the Legendre polynome of the phase function for each element of the Fourier series.

Output:

pxl [-kmu:kmu,knp] = atmospheric intrinsic reflectance

KERNEL_PBP: Computes the aerosol phase function and the components of the Legendre polynome of the rayleigh phase function. Based on the original subroutine KERNEL.f of 6S.

Input:

pbetal[0:knt,0:knang] = coefficients of the Legendre polynome.
 ppsl[klon,0:knang,-1:knang,-kmu:kmu]=components of the Legendre polynome of the phase function for each element of the Fourier series.

Output:

pxpl [-kmu:kmu] = components of the Legendre polynome of the rayleigh phase function for each element of the Fourier series.
 pbp [0:knt,0:kmu,-kmu:kmu] = aerosol phase function

SCATRA_GEMS: Computes the scattering transmission functions for the three atmospheric models, rayleigh, aerosol and mixture. Based on the original subroutine SCATRA.f of 6S.

Input:

pxmus = cosine of solar zenith angle
 pxmuv = cosine of viewing zenith angle
 ptodaer = total aerosol optical depth
 ptodray = total molecular optical depth
 ptamoy [0:knt] = aerosol optical thickness profile (truncated in discom.f)
 ptray[0:knt,] = rayleigh optical thickness profile
 pgb [klon,-kmu:kmu] = Gaussian weights for the zenith
 pizmoy[0:knt] = corrected scattering albedo

$\text{pbetal}[0:\text{knt},0:\text{knang}]$ = coefficients of the Legendre polynome.
 $\text{ppsl}[\text{klon},0:\text{knang},-1:\text{knang},-\text{kmu}:\text{kmu}]$ =components of the Legendre polynome of the phase function for each element of the Fourier series.
 $\text{prm} [-\text{kmu}:\text{kmu}]$ = Gaussian zenithal angles [in cosine]

Output:

$\text{prm} [-\text{kmu}:\text{kmu}]$ = Gaussian zenithal angles [in cosine]
 $\text{pddirtt}, \text{pddirtr}, \text{pddirta}$ = total, rayleigh and aerosol direct downward transmittance.
 $\text{pddifft}, \text{pddiftr}, \text{pddifta}$ = total, rayleigh and aerosol diffuse downward transmittance.
 $\text{pudirtt}, \text{pudirtr}, \text{pudirta}$ = total, rayleigh and aerosol direct upward transmittance.
 $\text{pudifft}, \text{pudiftr}, \text{pudifta}$ = total, rayleigh and aerosol diffuse upward transmittance.
 $\text{psphalbt}, \text{psphalbr}, \text{psphalba}$ = total, rayleigh and aerosol spherical albedo

CSALBR_GEMS: Calculates the spherical albedo of the molecular layer. Based on the subroutine CSALBR.f of 6S.

Input:

ptodray = total molecular optical depth

Output:

palb = rayleigh spherical albedo

ISO_GEMS: Computes the atmospheric transmission. Based on the original subroutine ISO.f of 6S.

Input:

ptodaer = total aerosol optical depth
 ptodray = total molecular optical depth
 $\text{prm} [-\text{kmu}:\text{kmu}]$ = Gaussian zenithal angles [in cosine]
 $\text{pgb} [\text{klon},-\text{kmu}:\text{kmu}]$ = Gaussian weights for the zenith
 $\text{ptamoy} [0:\text{knt}]$ = aerosol optical thickness profile (truncated in discom.f)
 $\text{ptray}[0:\text{knt},]$ = rayleigh optical thickness profile
 $\text{pizmoy}[0:\text{knt}]$ = corrected scattering albedo
 $\text{pbetal}[0:\text{knt},0:\text{knang}]$ = coefficients of the Legendre polynome.
 $\text{ppsl}[\text{klon},0:\text{knang},-1:\text{knang},-\text{kmu}:\text{kmu}]$ =components of the Legendre polynome of the phase function for each element of the Fourier series.

Output:

$\text{pxtrans}[-1:1]$ = atmospheric transmission

Appendix B: Validation figures

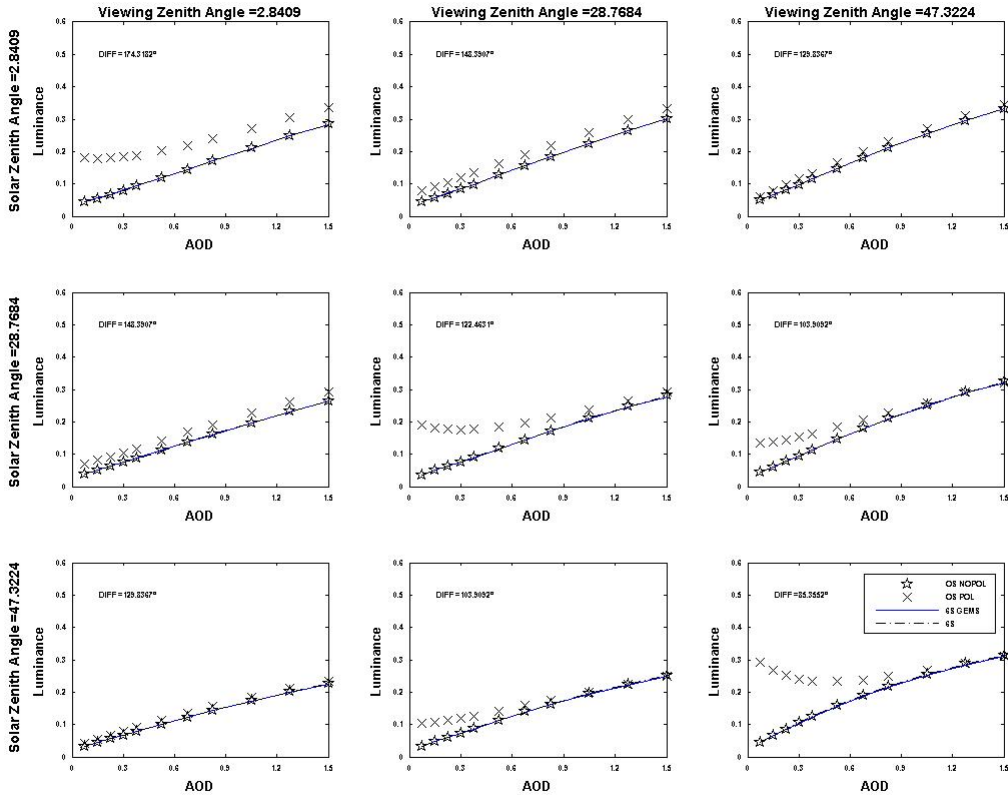


Figure B-1: Radiances according to 6S (black discontinuous), 6S GEMS (blue), OS (stars) and OS without polarization and glitter (black cross) for different solar and viewing zenith angles. The results correspond to a wavelength of 565 nm, a difference in azimuthal angle of 180°. The aerosol model corresponds to fine mode model 1 with a mean modal radius of 0.04, standard deviation of 0.46 and a refractive index of 1.35.

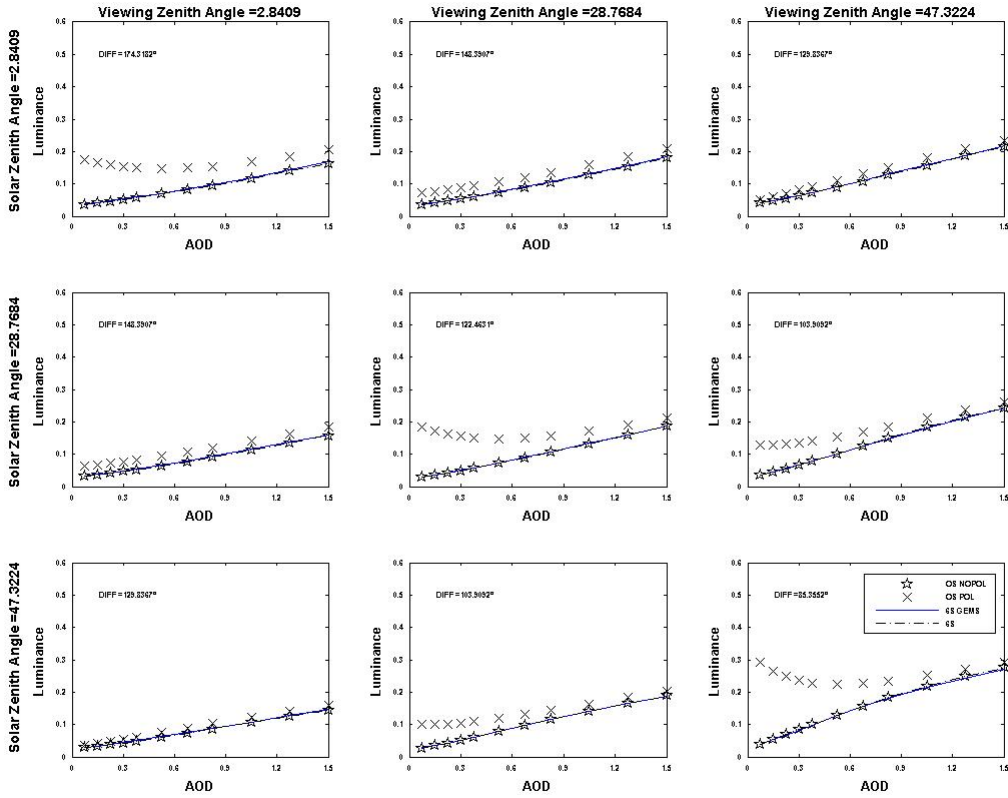


Figure B-2: Same as figure B-1 but for fine mode model 2 with a mean modal radius of 0.08, standard deviation of 0.46 and a refractive index of 1.35.

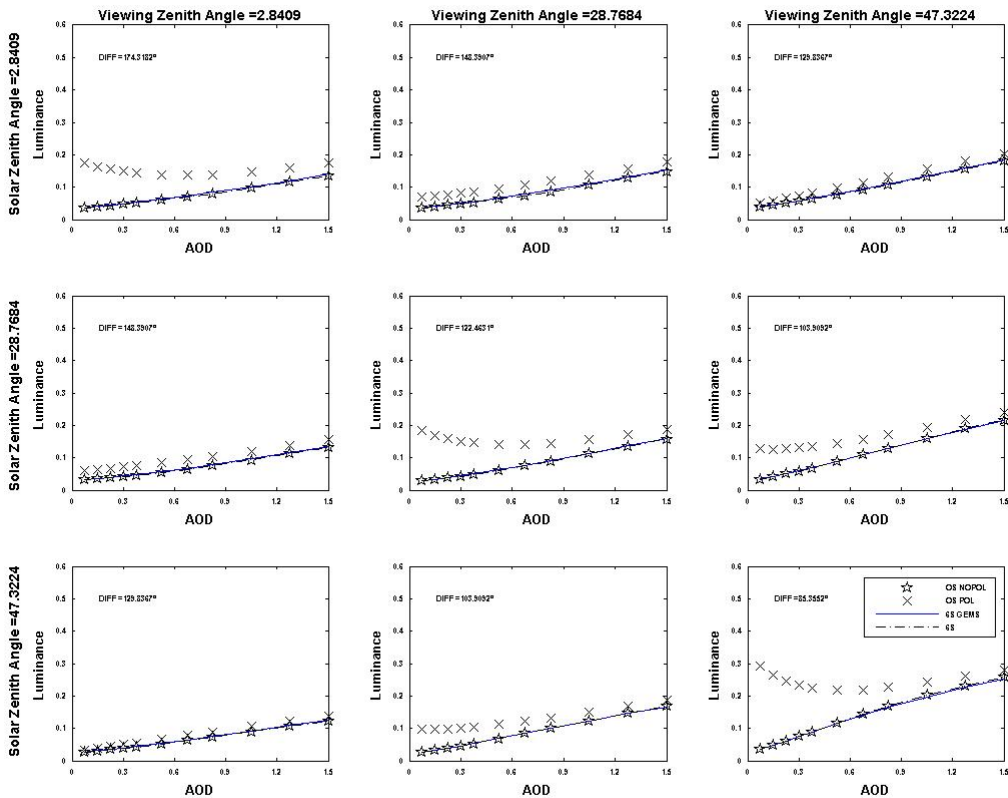


Figure B-3: Same as figure B-1 but for fine mode model 3 with a mean modal radius of 0.1, standard deviation of 0.46 and a refractive index of 1.35.

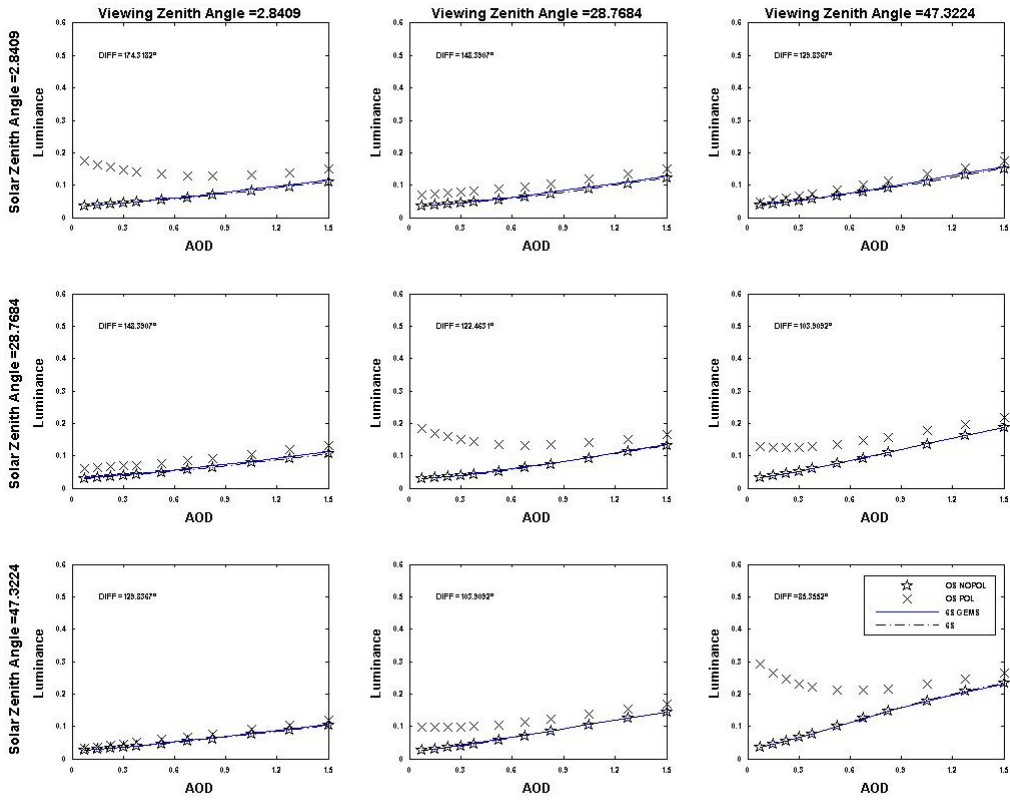


Figure B-4: Same as figure B-1 but for fine mode model 4 with a mean modal radius of 0.13, standard deviation of 0.46 and a refractive index of 1.35.

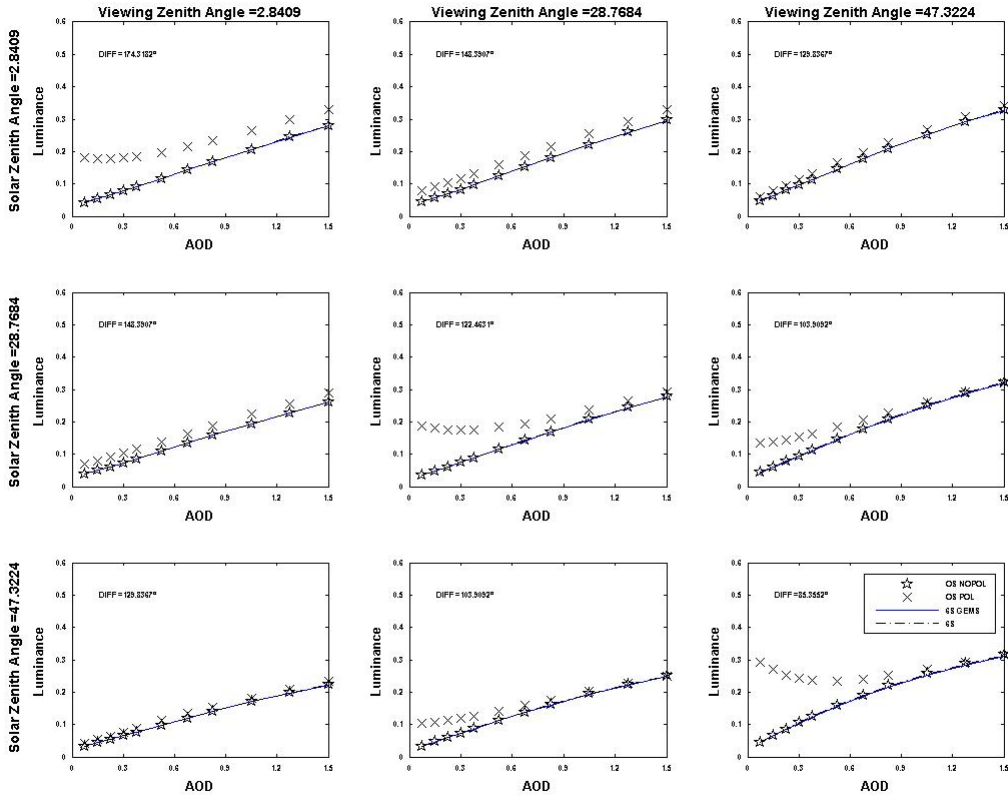


Figure B-5: Radiances according to 6S (black discontinuous), 6S GEMS (blue), OS (stars) and OS without polarization and glitter (black cross) for different solar and viewing zenithal angles. The results correspond to a wavelength of 565 nm, a difference in azimuthal angle of 180°. The aerosol model corresponds to fine mode model 1 with a mean modal radius of 0.04, standard deviation of 0.46 and a refractive index of 1.45.

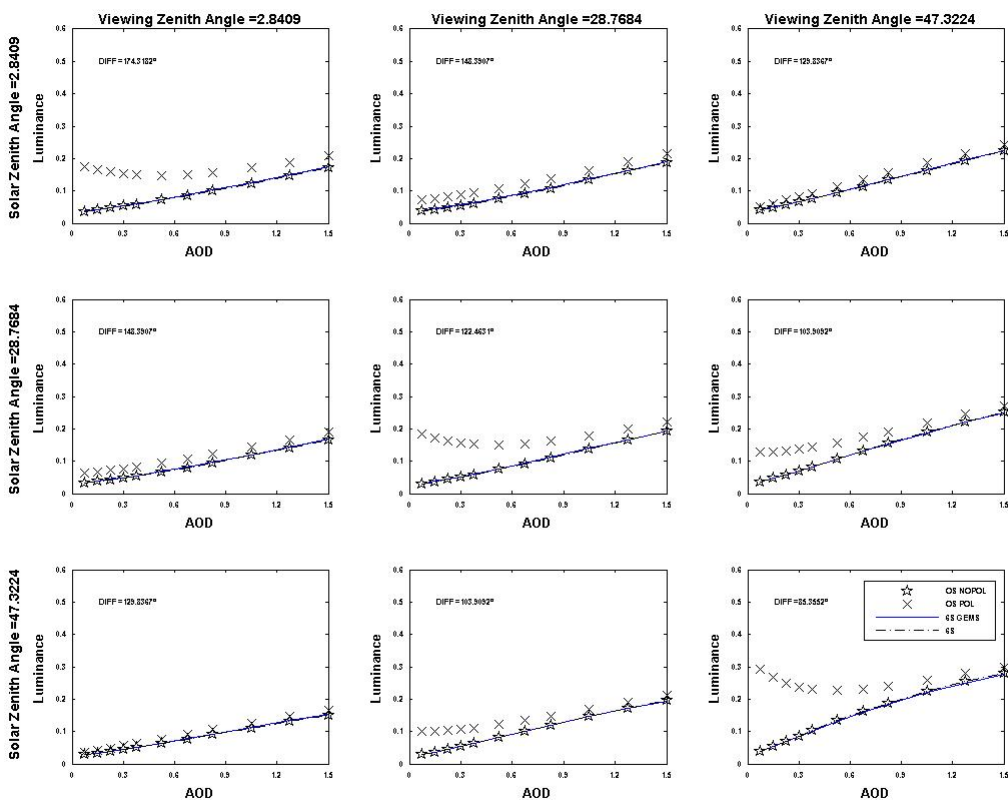


Figure B-6: Same as figure B-5 but for fine mode model 2 with a mean modal radius of 0.08, standard deviation of 0.46 and a refractive index of 1.45.

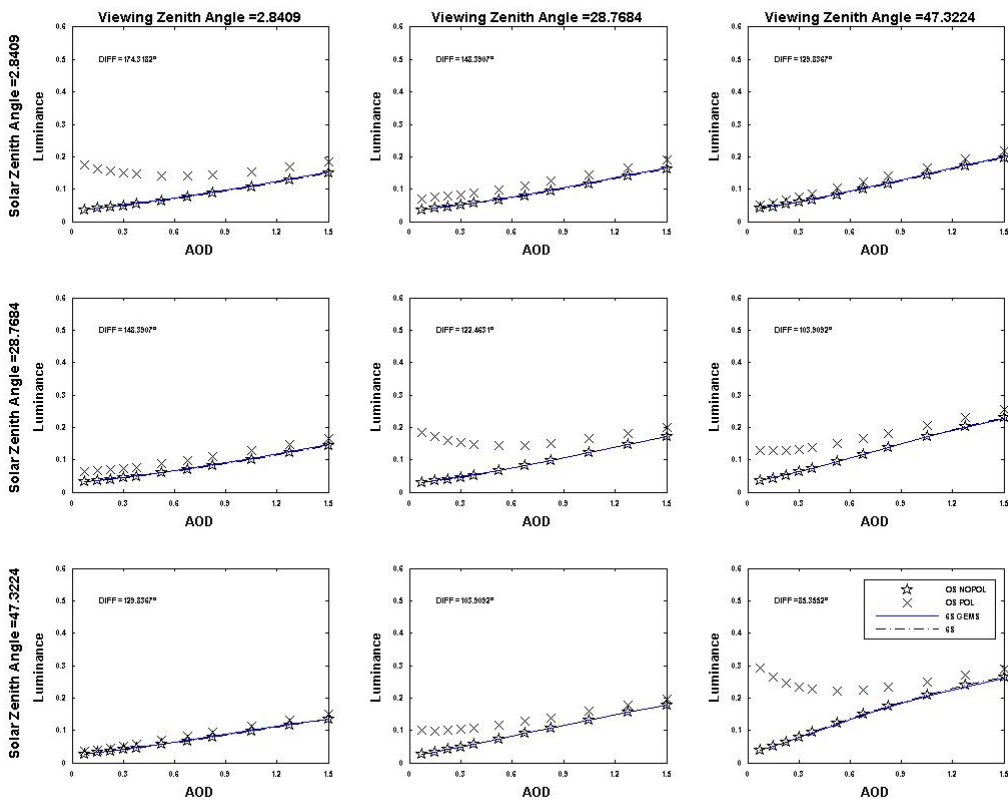


Figure B-7: Same as figure B-5 but for fine mode model 3 with a mean modal radius of 0.1, standard deviation of 0.46 and a refractive index of 1.45.

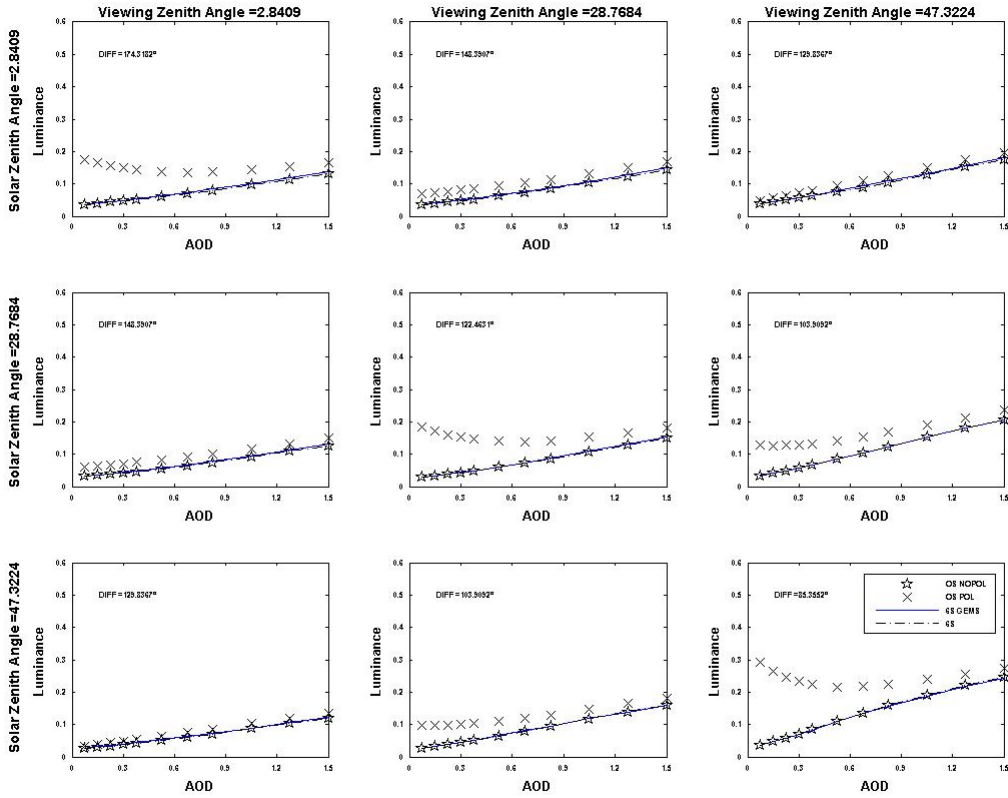


Figure B-8: Same as figure B-5 but for fine mode model 4 with a mean modal radius of 0.13, standard deviation of 0.46 and a refractive index of 1.45.

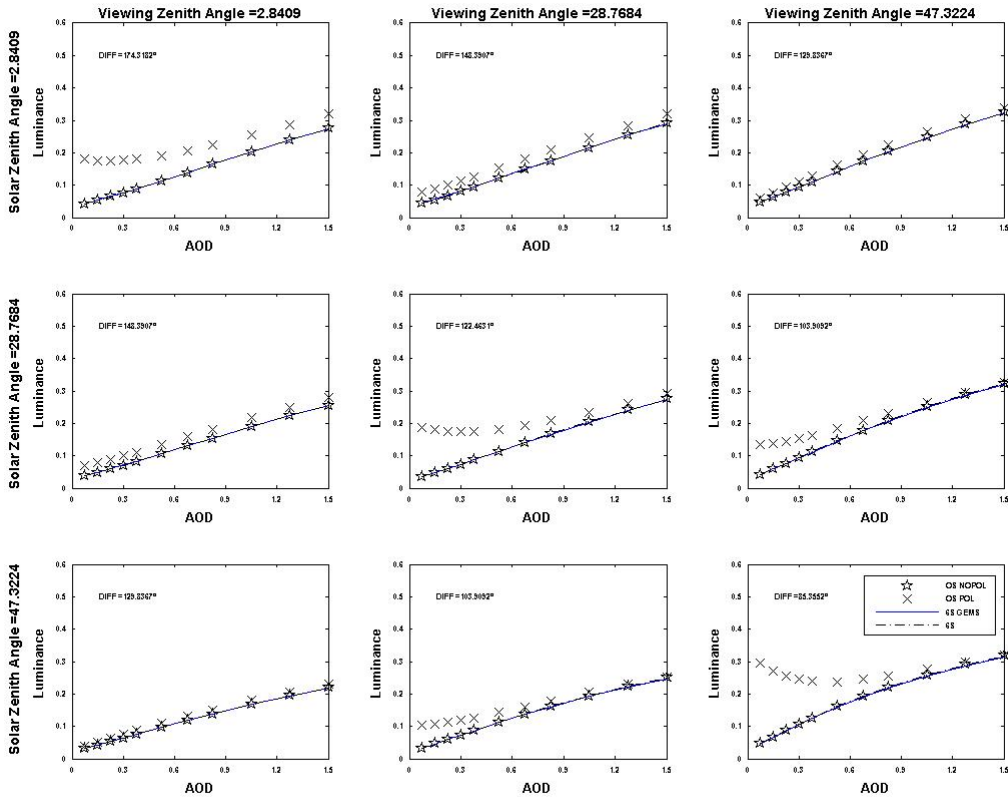


Figure B-9: Radiance according to 6S (black discontinuous), 6S GEMS (blue), OS (stars) and OS without polarization and glitter (black cross) for different solar and viewing zenithal angles. The results correspond to a wavelength of 565 nm, a difference in azimuthal angle of 180°. The aerosol model corresponds to fine mode model 1 with a mean modal radius of 0.04, standard deviation of 0.46 and a refractive index of 1.60.

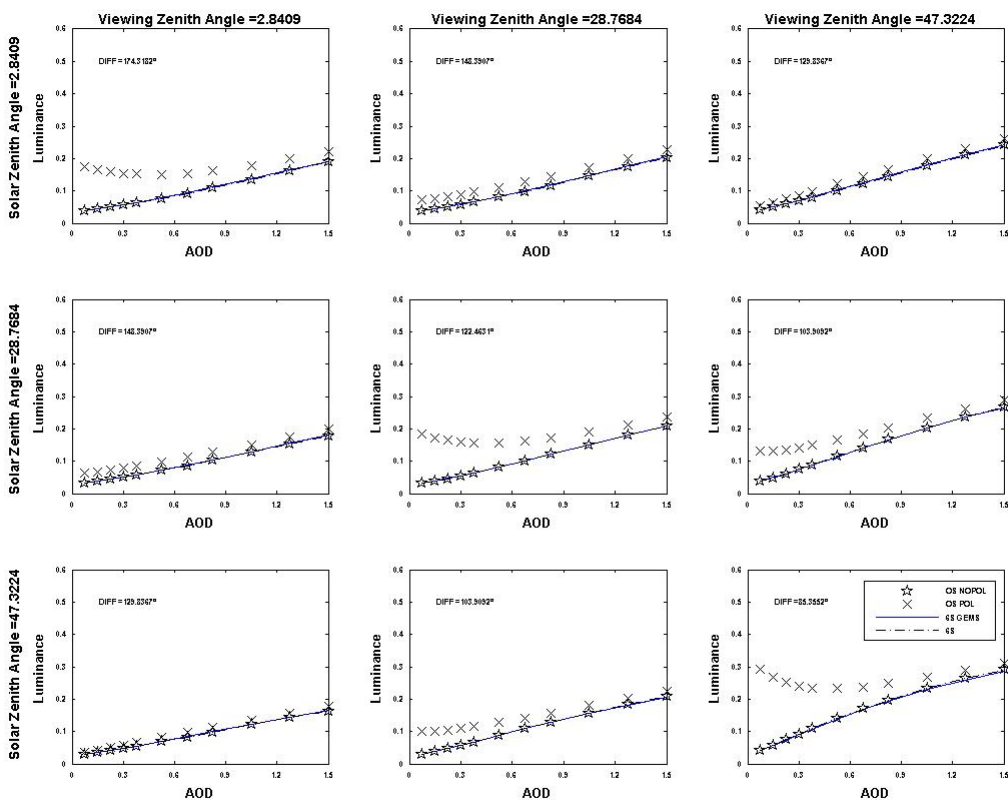


Figure B-10: Same as figure B-9 but for fine mode model 2 with a mean modal radius of 0.08, standard deviation of 0.46 and a refractive index of 1.60.

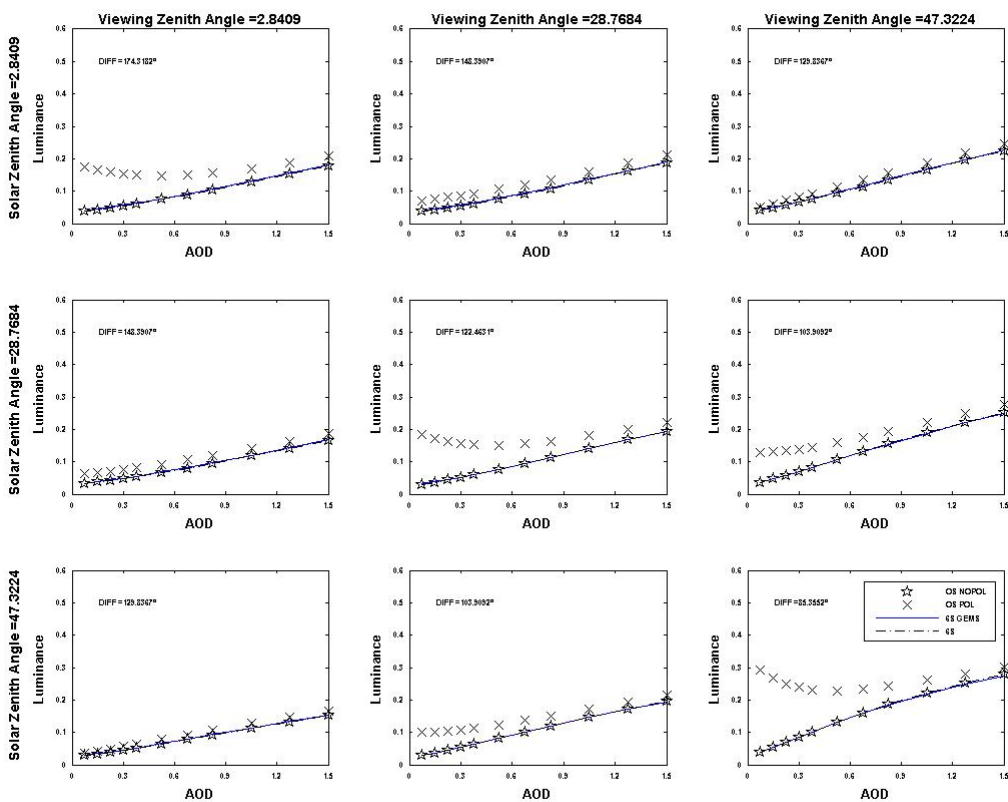


Figure B-11: Same as figure B-10 but for fine mode model 3 with a mean modal radius of 0.1, standard deviation of 0.46 and a refractive index of 1.60.

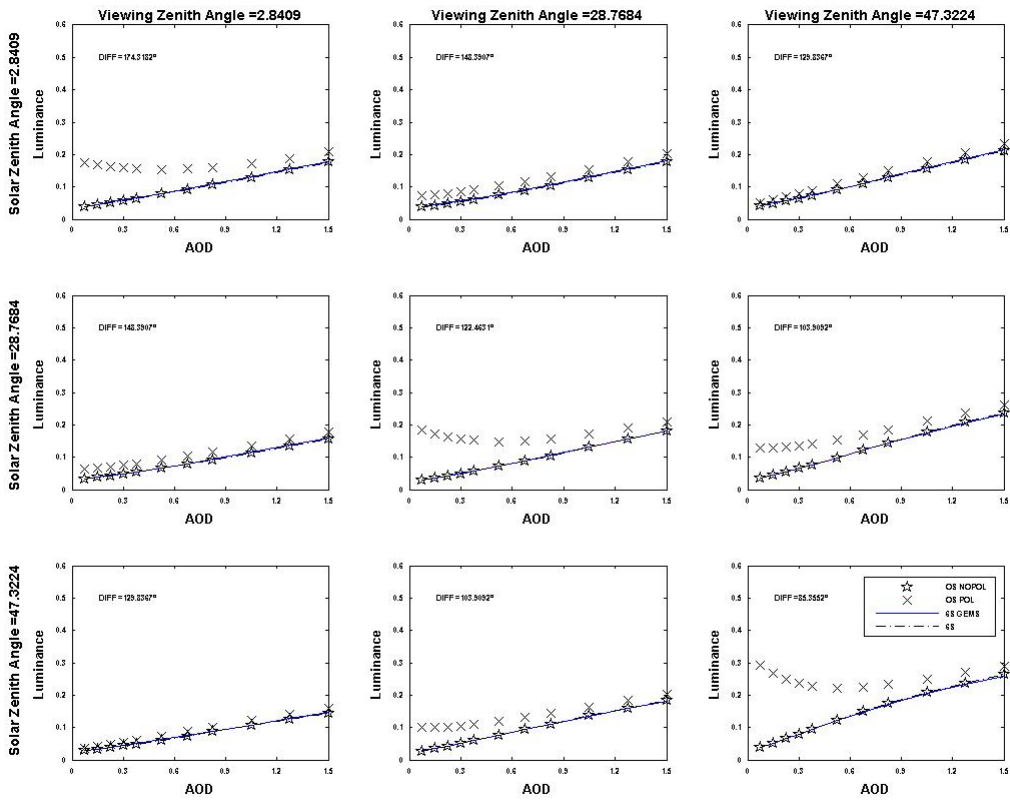


Figure B-12: Same as figure B-10 but for fine mode model 4 with a mean modal radius of 0.13, standard deviation of 0.46 and a refractive index of 1.60.

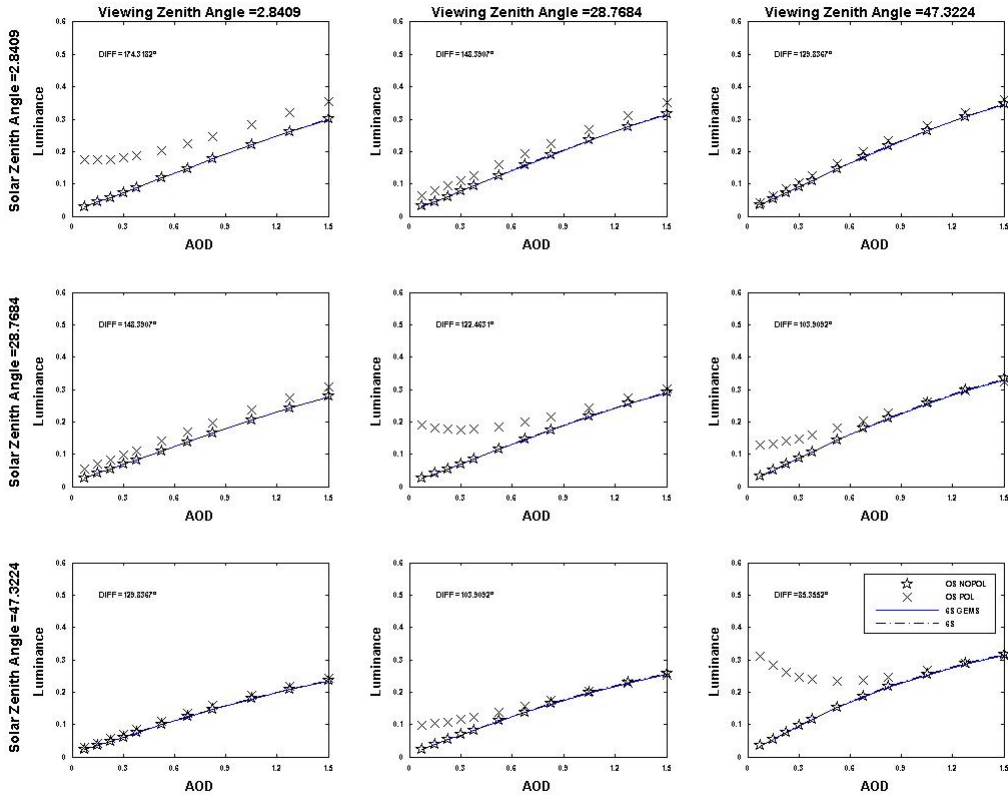


Figure B-13: Radiances according to 6S (black discontinuous), 6S GEMS (blue), OS (stars) and OS without polarization and glitter (black cross) for different solar and viewing zenithal angles. The results correspond to a wavelength of 670 nm, a difference in azimuthal angle of 180°. The aerosol model corresponds to fine mode model 1 with a mean modal radius of 0.04, standard deviation of 0.46 and a refractive index of 1.35.

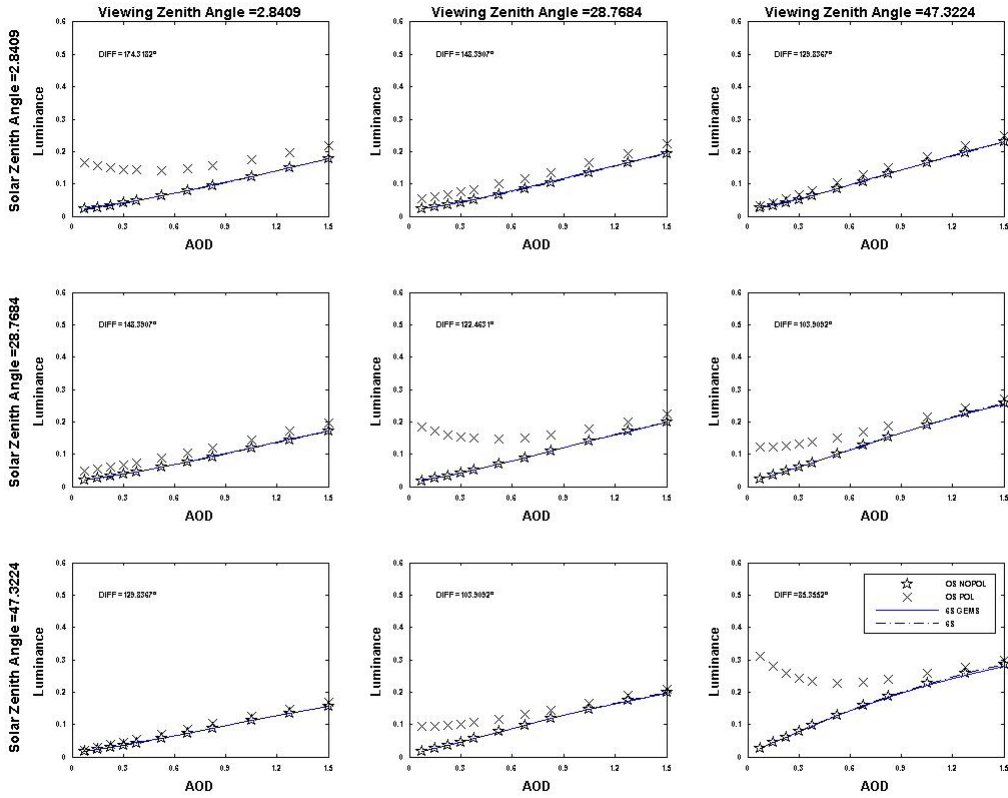


Figure B-14: Same as figure B-13 but for fine mode model 2 with a mean modal radius of 0.08, standard deviation of 0.46 and a refractive index of 1.35.

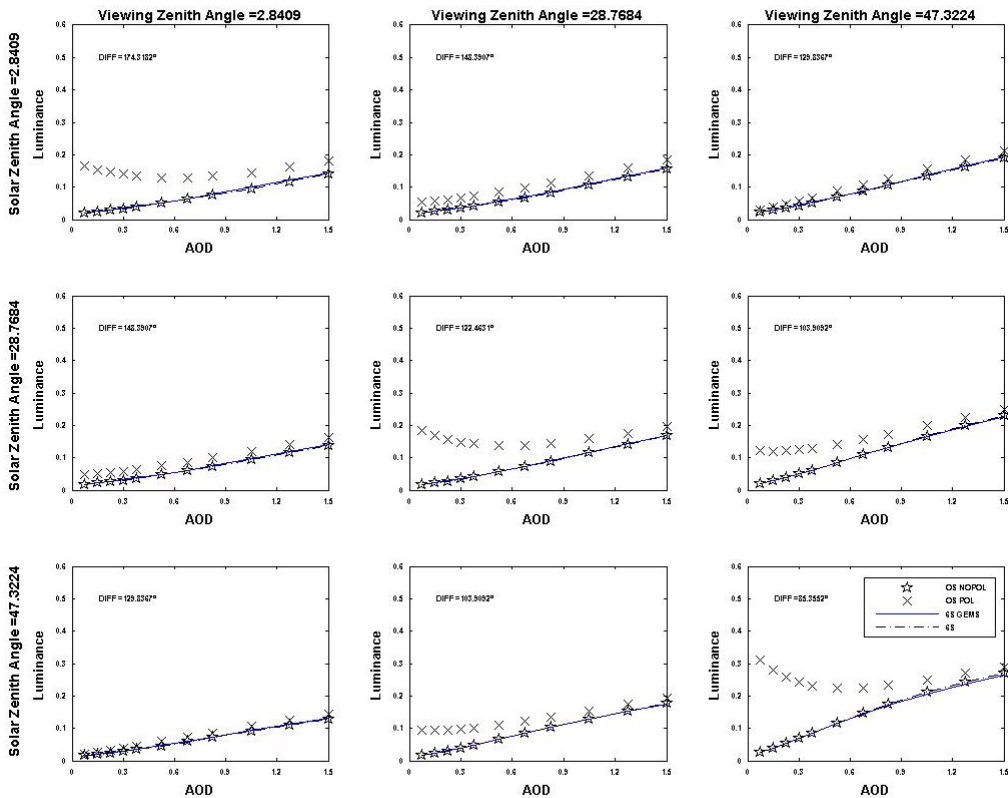


Figure B-15: Same as figure B-13 but for fine mode model 3 with a mean modal radius of 0.1, standard deviation of 0.46 and a refractive index of 1.35.

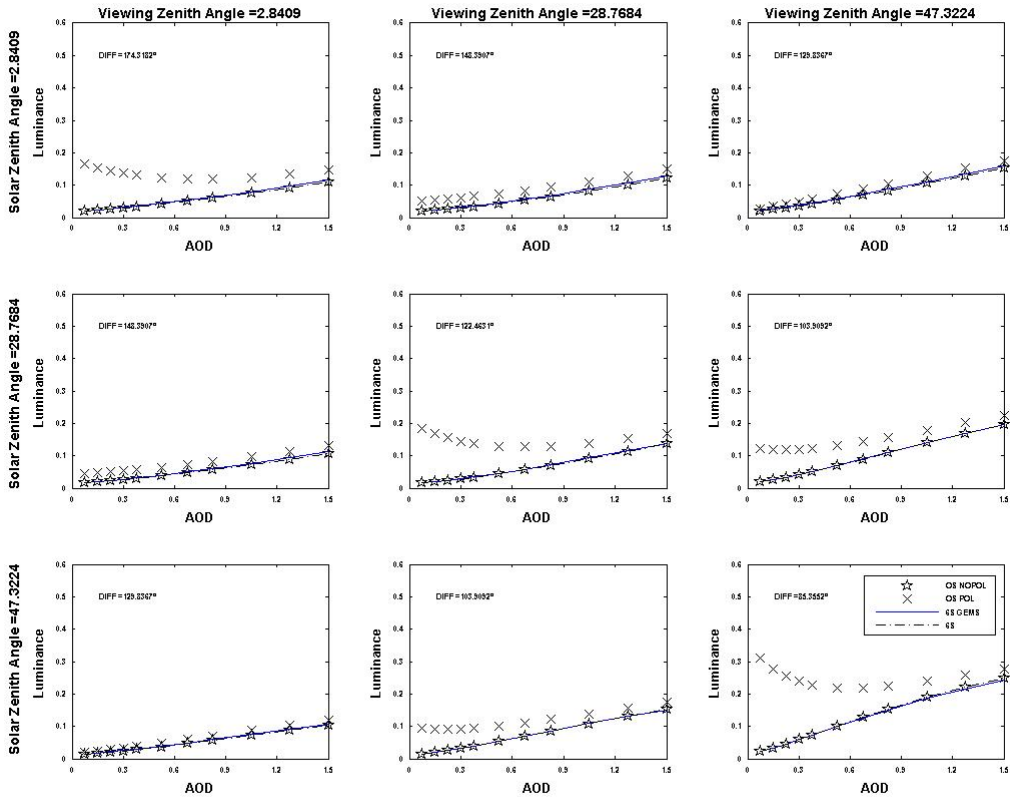


Figure B-16: Same as figure B-13 but for fine mode model 4 with a mean modal radius of $0.13 \mu\text{m}$, standard deviation of 0.46 and a refractive index of 1.35 .

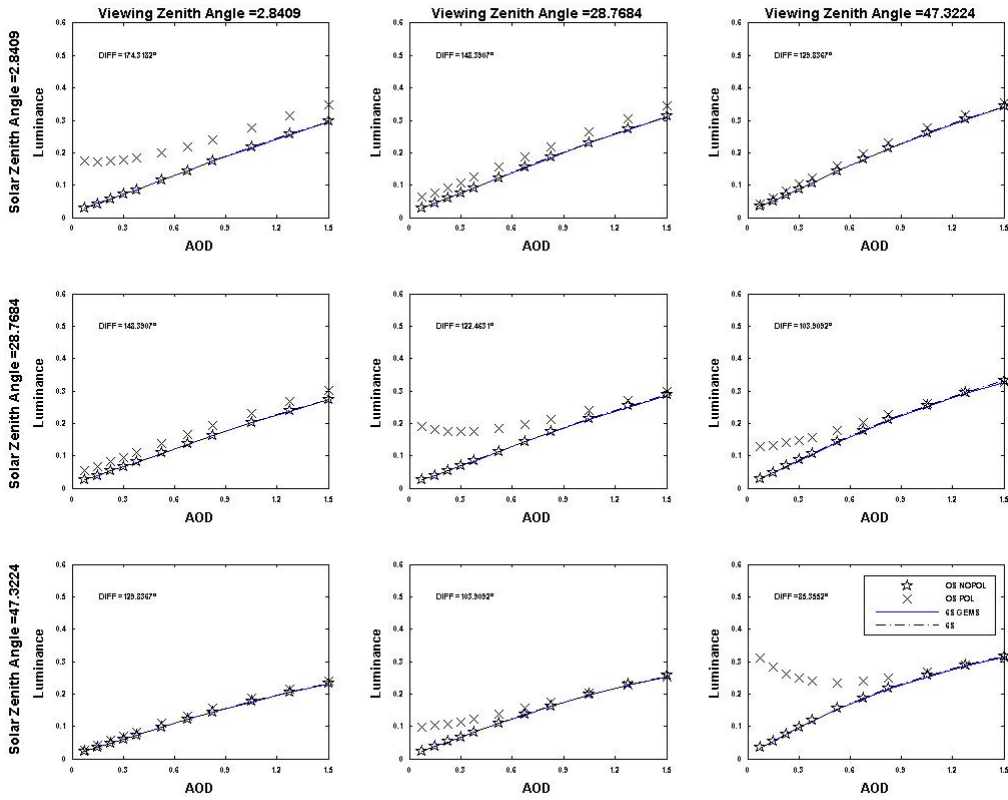


Figure B-17: Radiances according to 6S (black discontinuous), 6S GEMS (blue), OS (stars) and OS without polarization and glitter (black cross) for different solar and viewing zenithal angles. The results correspond to a wavelength of 670 nm, a difference in azimuthal angle of 180°. The aerosol model corresponds to fine mode model 1 with a mean modal radius of 0.04 μm , standard deviation of 0.46 and a refractive index of 1.45.

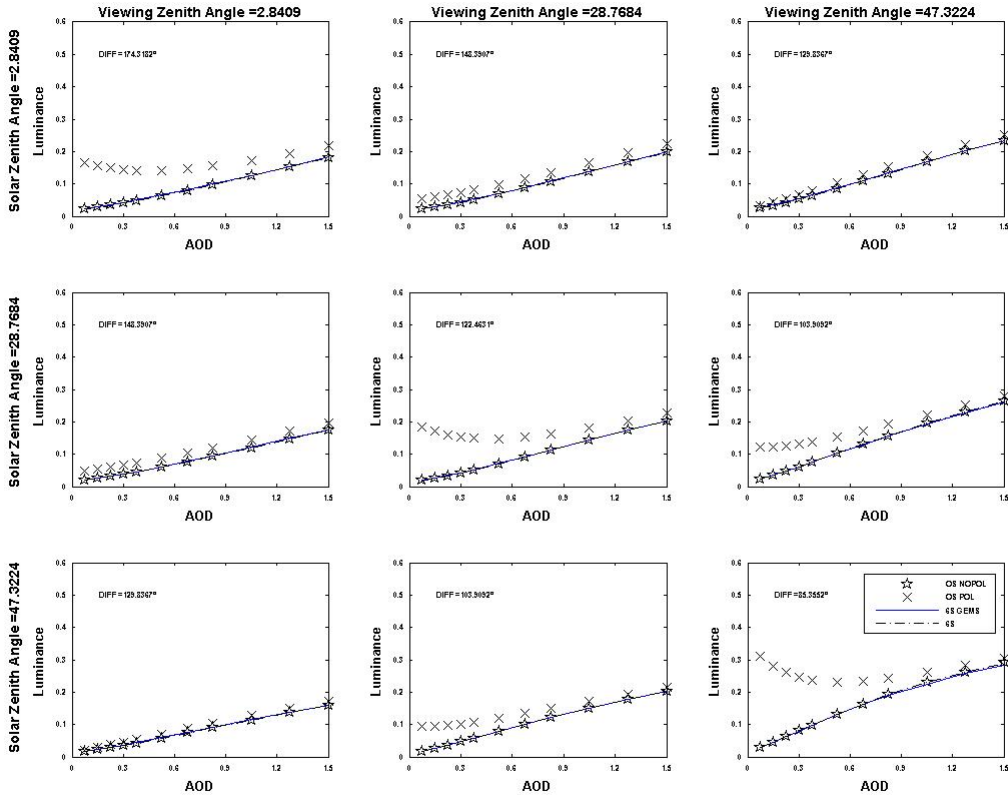


Figure B-18: Same as figure B-17 but for fine mode model 2 with a mean modal radius of $0.08 \mu\text{m}$, standard deviation of 0.46 and a refractive index of 1.45 .

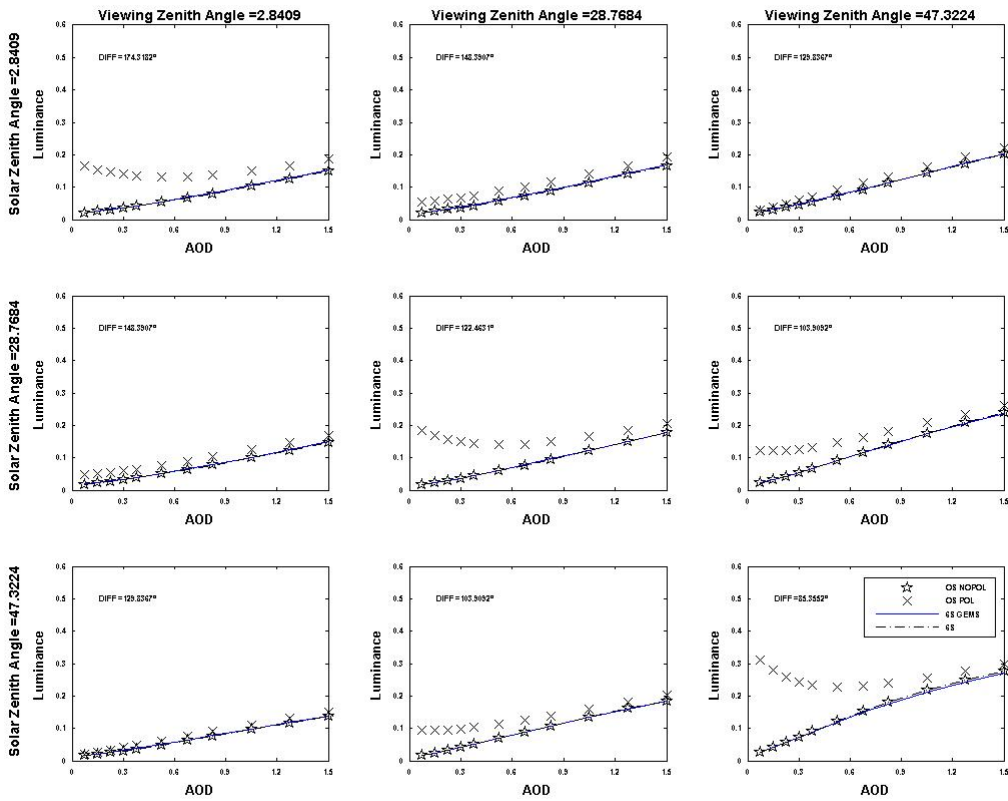


Figure B-19: Same as figure B-17 but for fine mode model 3 with a mean modal radius of $0.1 \mu\text{m}$, standard deviation of 0.46 and a refractive index of 1.45 .

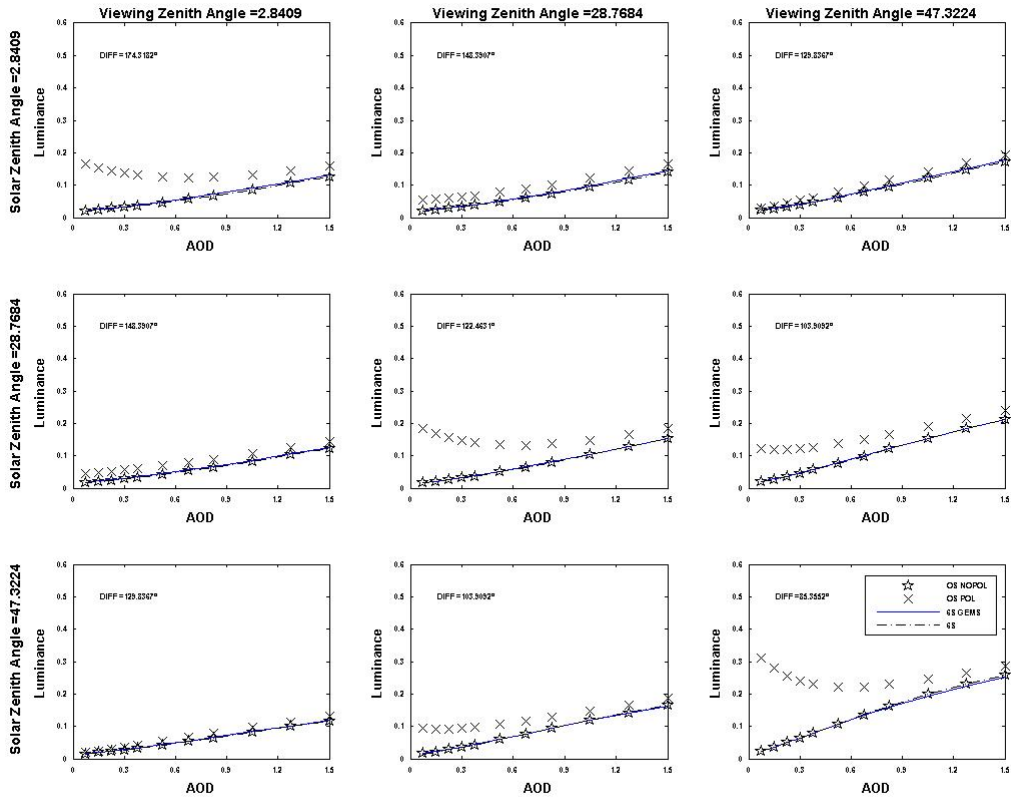


Figure B-20: Same as figure B-17 but for fine mode model 4 with a mean modal radius of $0.13 \mu\text{m}$, standard deviation of 0.46 and a refractive index of 1.45 .

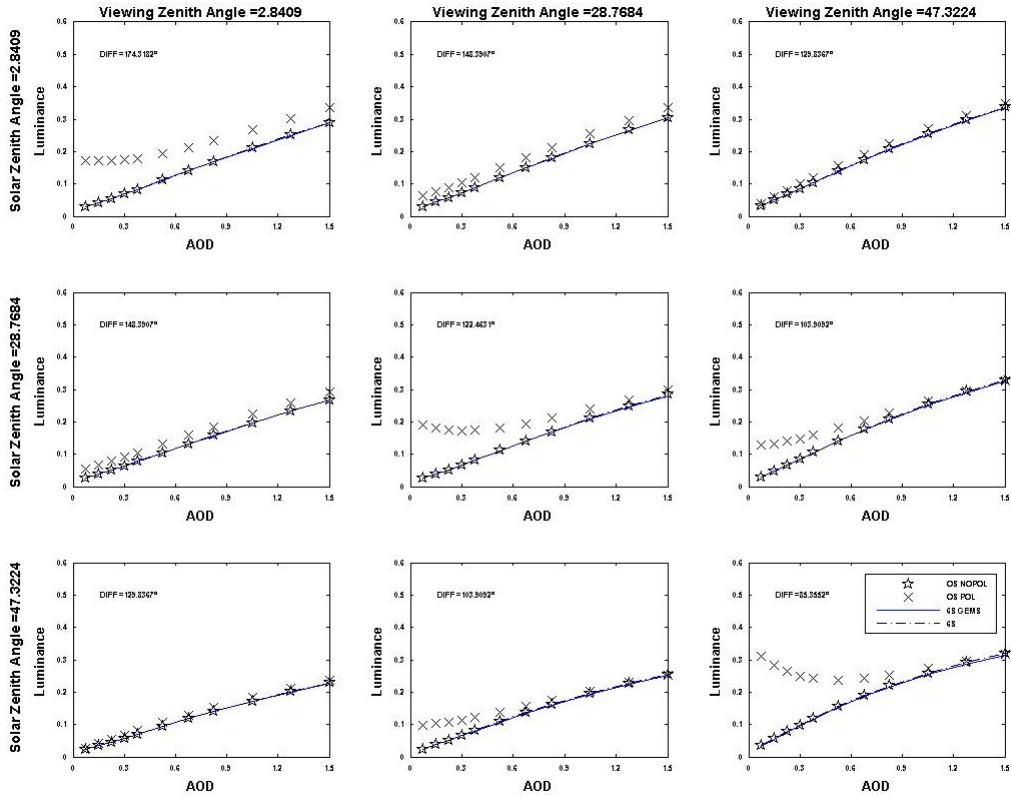


Figure B-21: Radiances according to 6S (black discontinuous), 6S GEMS (blue), OS (stars) and OS without polarization and glitter (black cross) for different solar and viewing zenithal angles. The results correspond to a wavelength of 670 nm, a difference in azimuthal angle of 180°. The aerosol model corresponds to fine mode model 1 with a mean modal radius of 0.04 μm , standard deviation of 0.46 and a refractive index of 1.60.

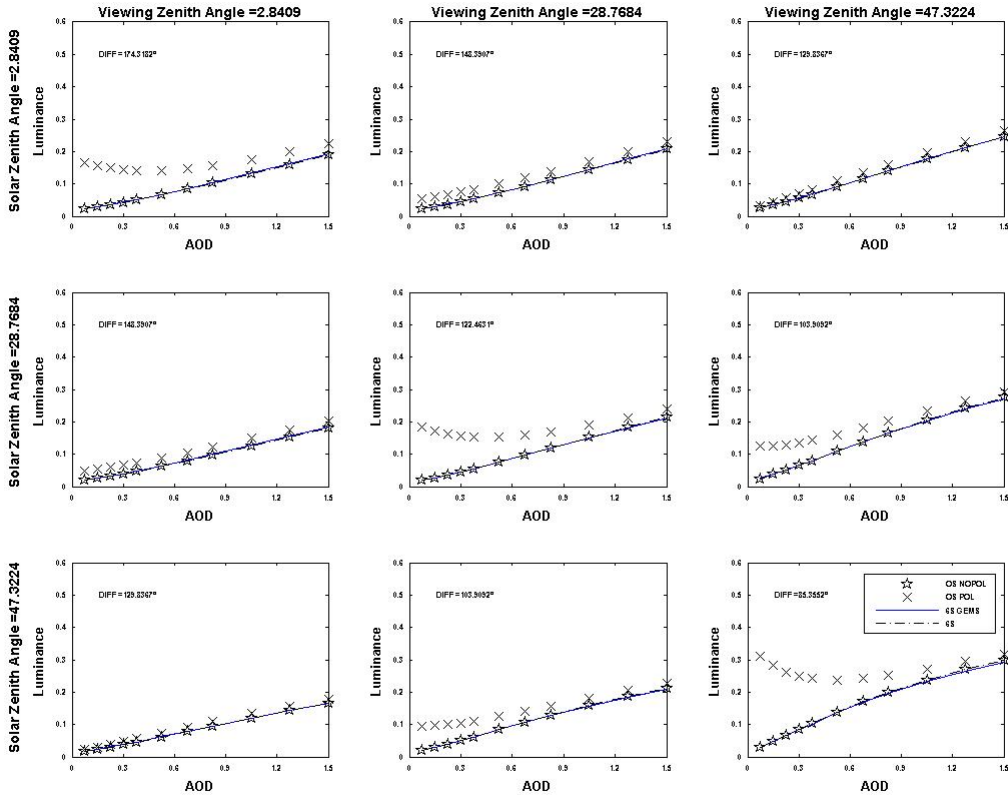


Figure B-22: Same as figure B-21 but for fine mode model 2 with a mean modal radius of $0.08 \mu\text{m}$, standard deviation of 0.46 and a refractive index of 1.60 .

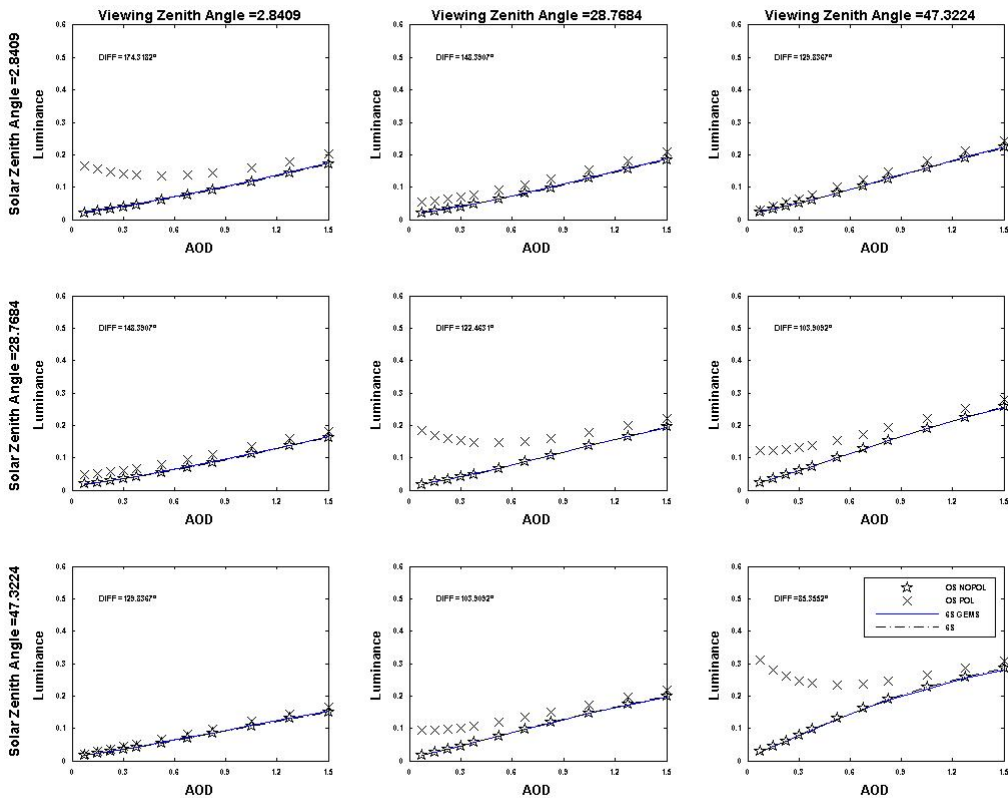


Figure B-23: Same as figure B-21 but for fine mode model 3 with a mean modal radius of $0.1 \mu\text{m}$, standard deviation of 0.46 and a refractive index of 1.60 .

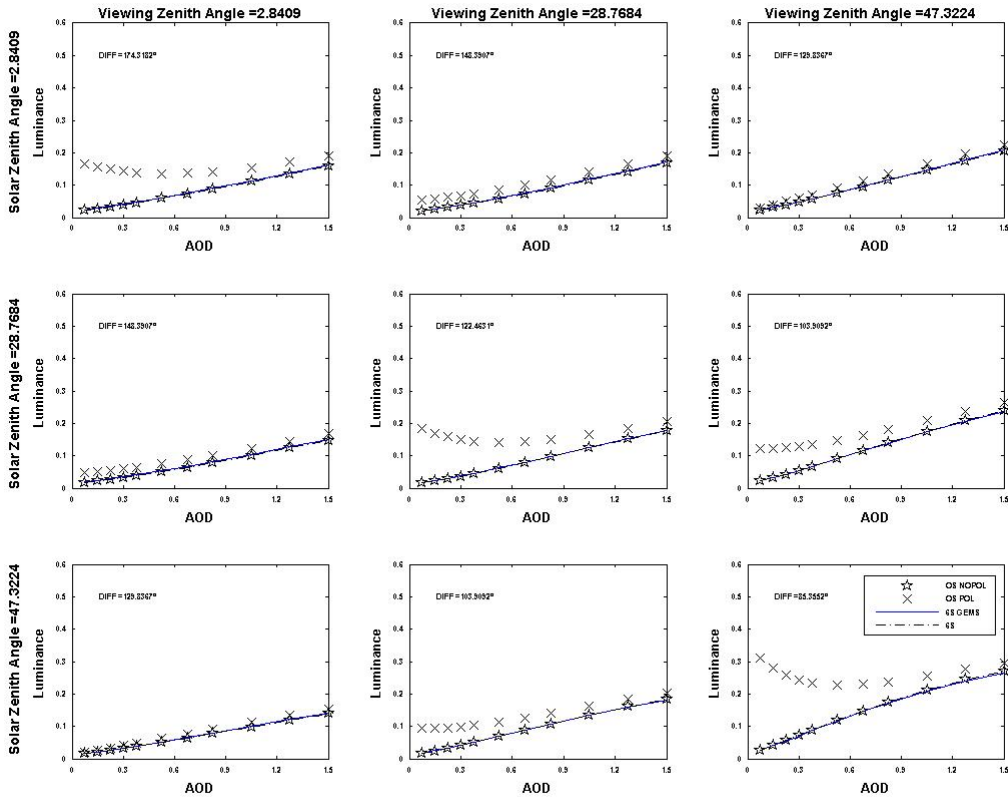


Figure B-24: Same as figure B-21 but for fine mode model 4 with a mean modal radius of 0.13 μm , standard deviation of 0.46 and a refractive index of 1.60.

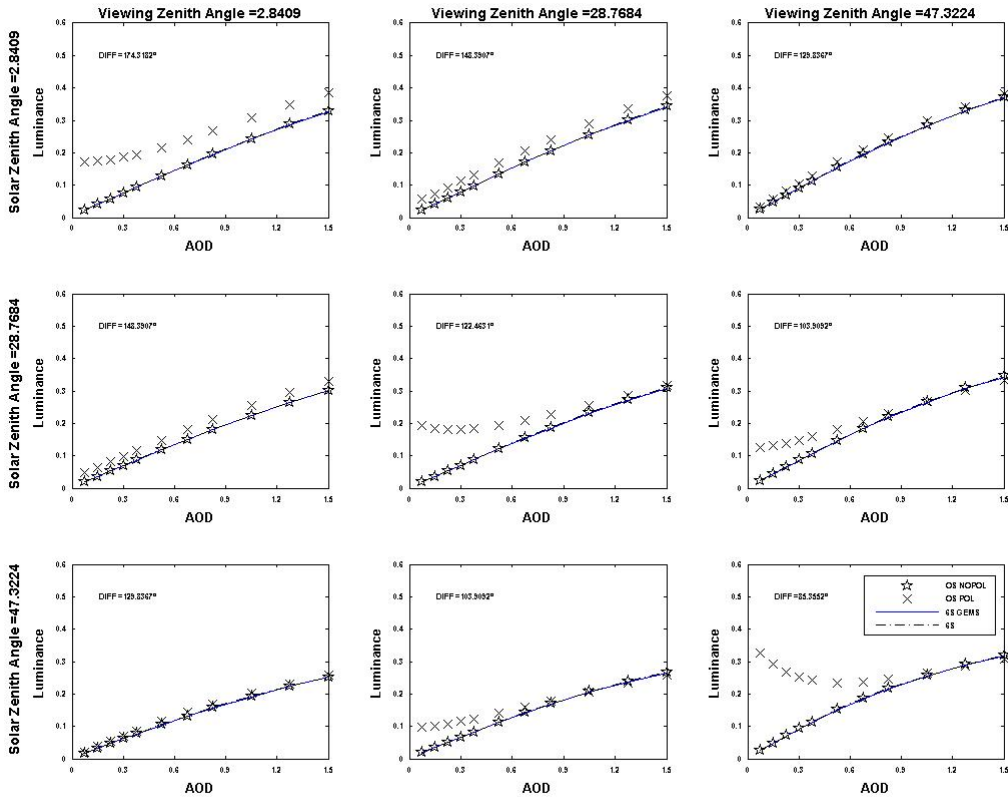


Figure B-25: Radiance according to 6S (black discontinuous), 6S GEMS (blue), OS (stars) and OS without polarization and glitter (black cross) for different solar and viewing zenithal angles. The results correspond to a wavelength of 865 nm, a difference in azimuthal angle of 180°. The aerosol model corresponds to fine mode model 1 with a mean modal radius of 0.04 μm , standard deviation of 0.46 and a refractive index of 1.35.

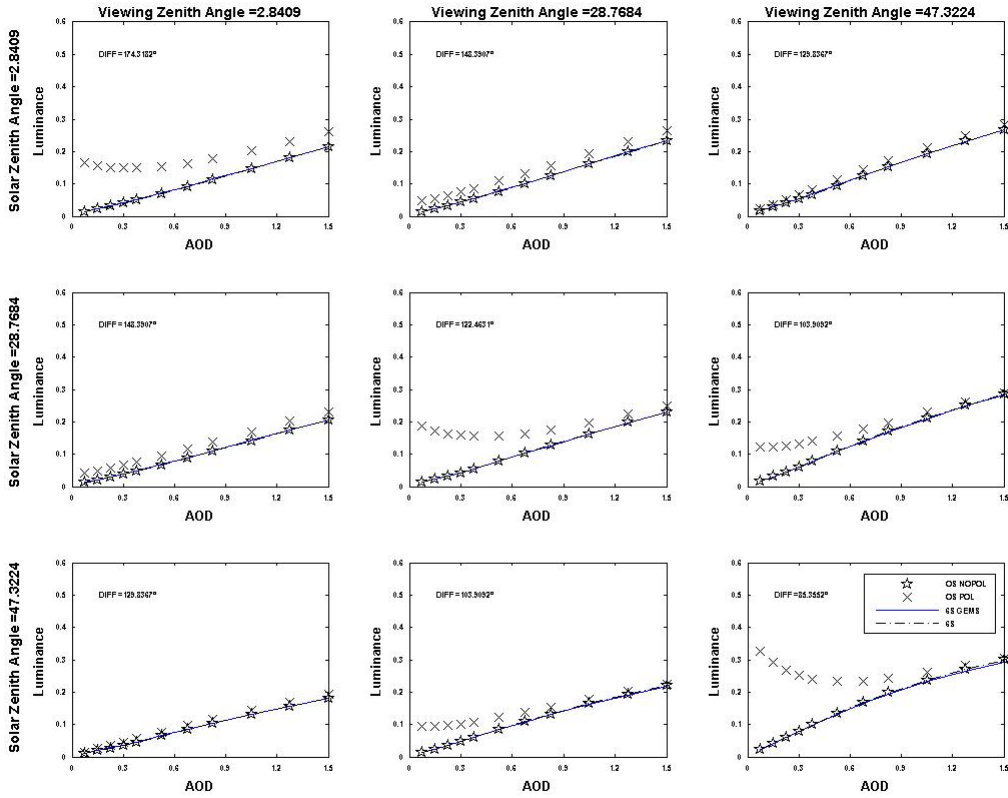


Figure B-26: Same as figure B-25 but for fine mode model 2 with a mean modal radius of $0.08 \mu\text{m}$, standard deviation of 0.46 and a refractive index of 1.35 .

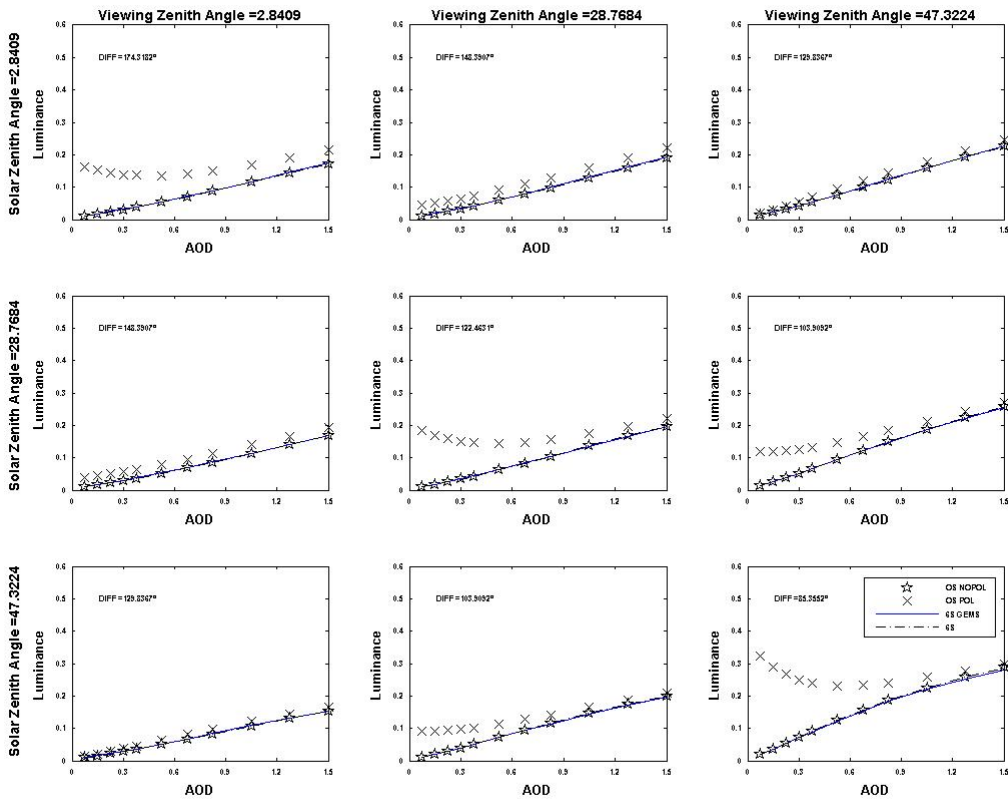


Figure B-27: Same as figure B-25 but for fine mode model 3 with a mean modal radius of $0.1 \mu\text{m}$, standard deviation of 0.46 and a refractive index of 1.35 .

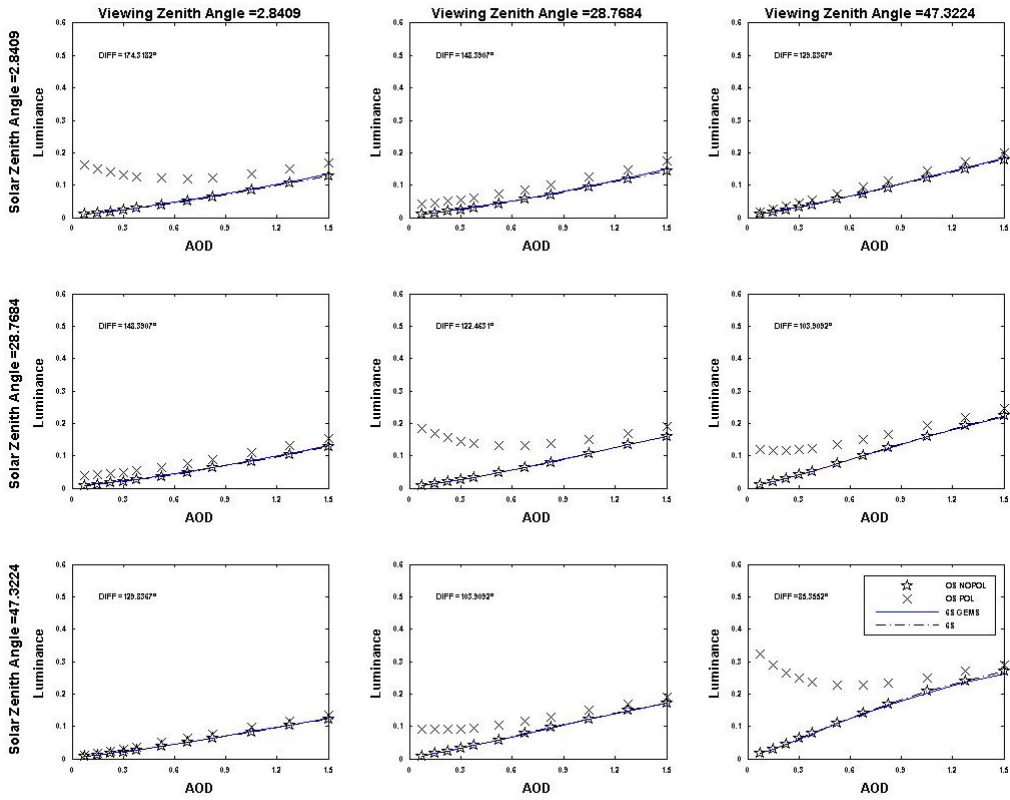


Figure B-28: Same as figure B-25 but for fine mode model 4 with a mean modal radius of $0.13 \mu\text{m}$, standard deviation of 0.46 and a refractive index of 1.35 .

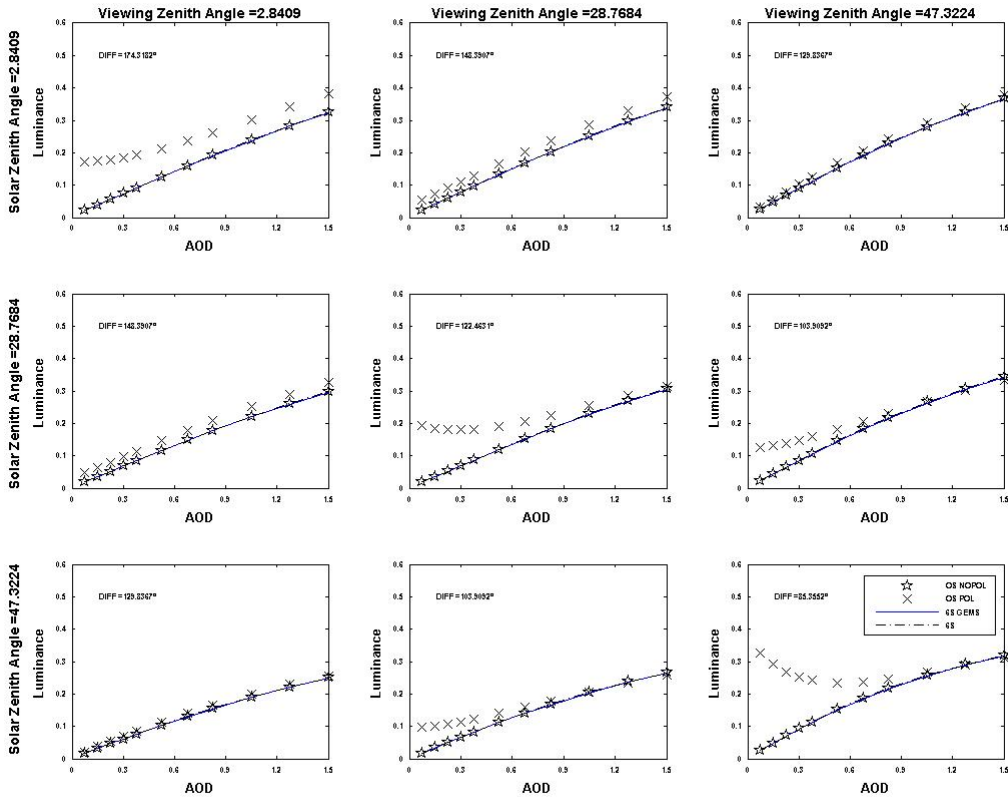


Figure B-29: Radiance according to 6S (black discontinuous), 6S GEMS (blue), OS (stars) and OS without polarization and glitter (black cross) for different solar and viewing zenithal angles. The results correspond to a wavelength of 865 nm, a difference in azimuthal angle of 180°. The aerosol model corresponds to fine mode model 1 with a mean modal radius of 0.04 μm , standard deviation of 0.46 and a refractive index of 1.45.

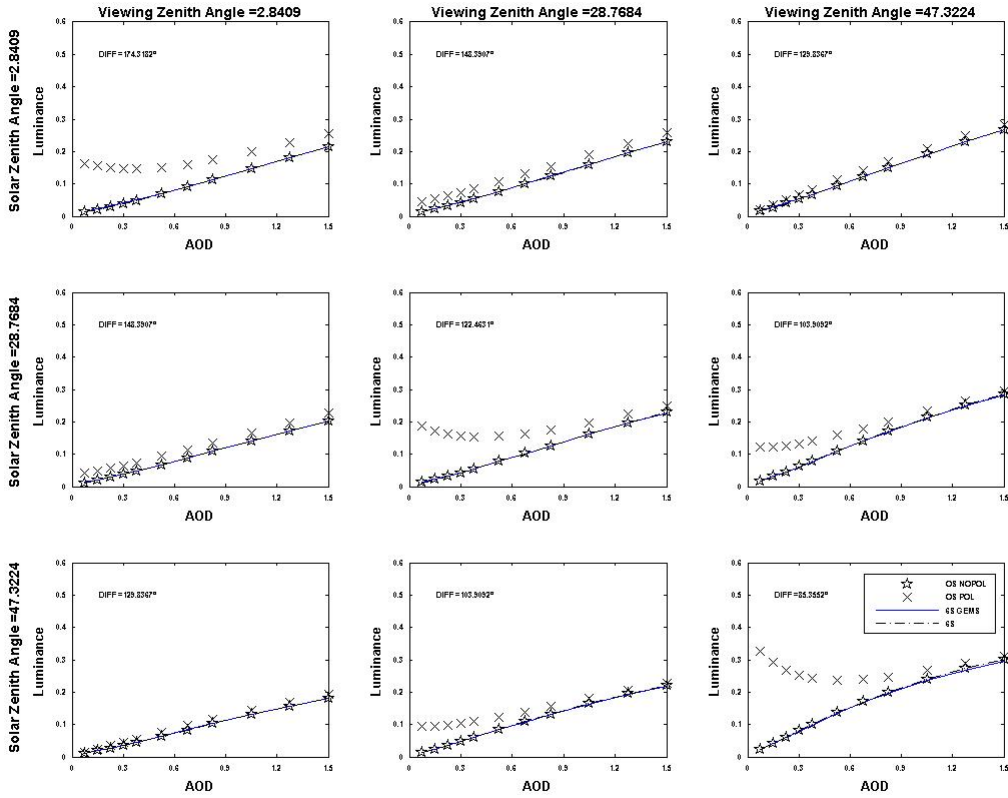


Figure B-30: Same as figure B-29 but for fine mode model 2 with a mean modal radius of $0.08 \mu\text{m}$, standard deviation of 0.46 and a refractive index of 1.45 .

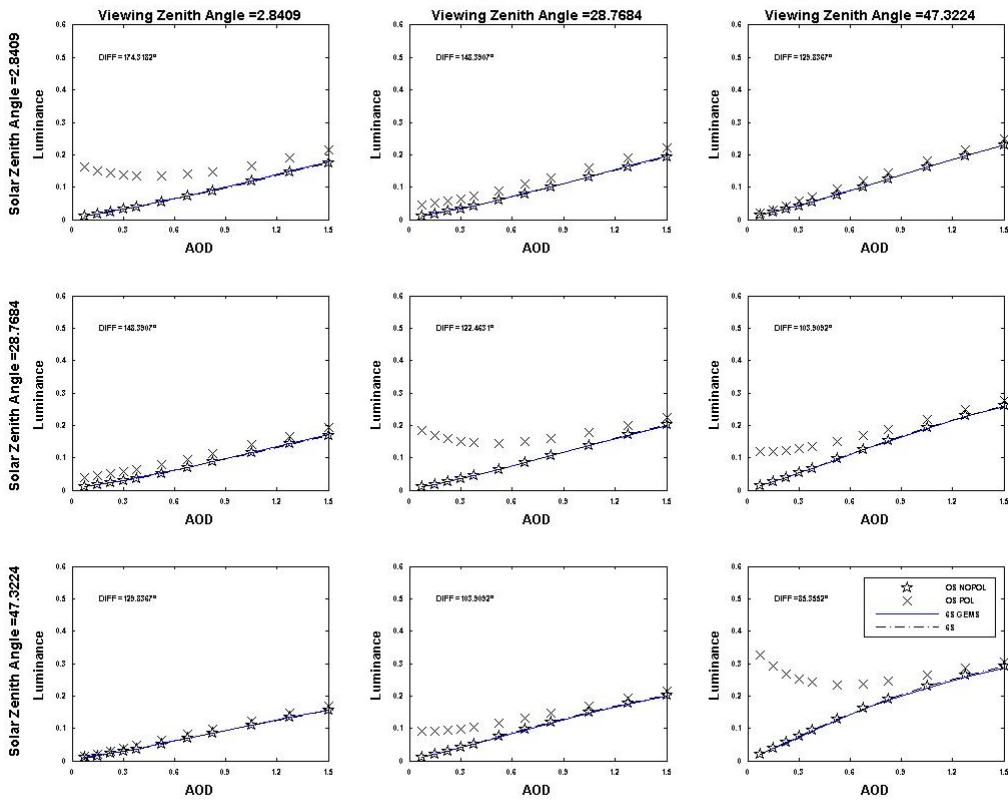


Figure B-31: Same as figure B-29 but for fine mode model 3 with a mean modal radius of $0.1 \mu\text{m}$, standard deviation of 0.46 and a refractive index of 1.45 .

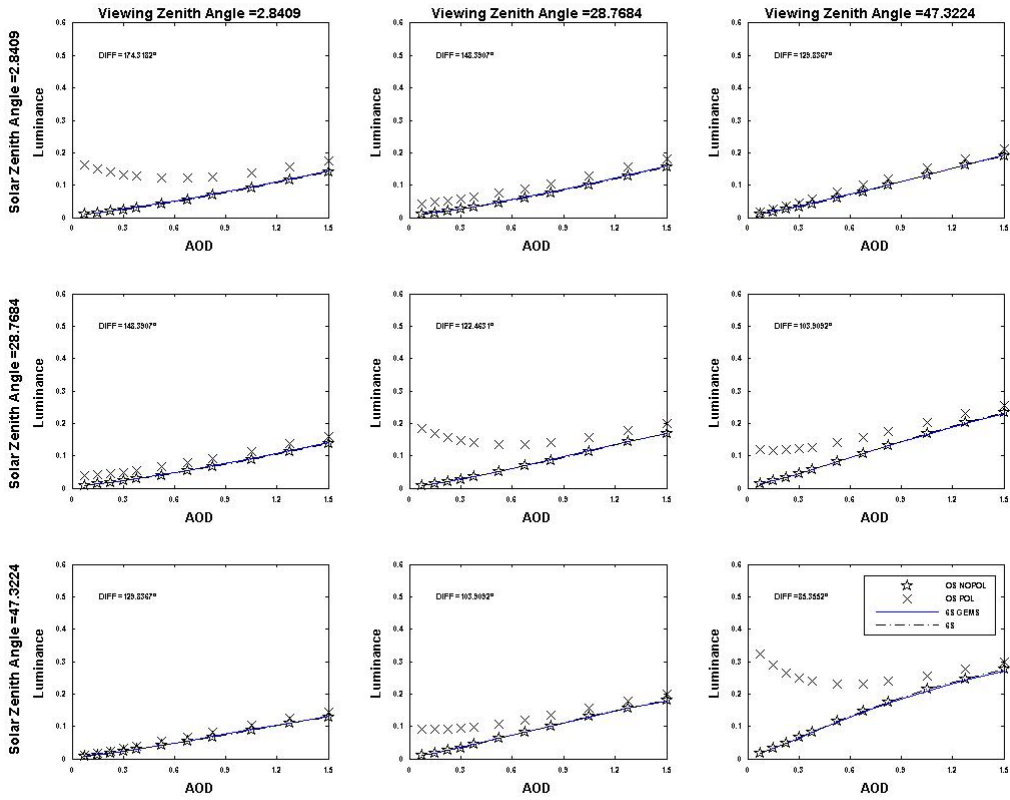


Figure B-32: Same as figure B-29 but for fine mode model 4 with a mean modal radius of 0.13 μm , standard deviation of 0.46 and a refractive index of 1.45.

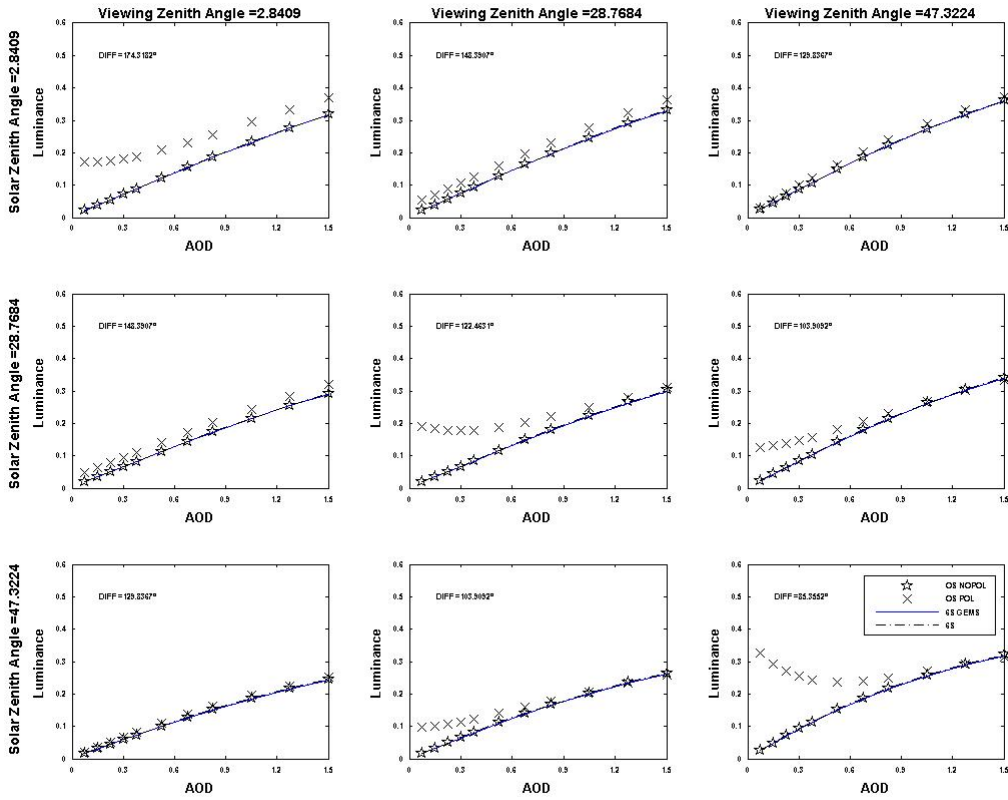


Figure B-33: Radiance according to 6S (black discontinuous), 6S GEMS (blue), OS (stars) and OS without polarization and glitter (black cross) for different solar and viewing zenithal angles. The results correspond to a wavelength of 865 nm, a difference in azimuthal angle of 180°. The aerosol model corresponds to fine mode model 1 with a mean modal radius of 0.04 μm , standard deviation of 0.46 and a refractive index of 1.60.

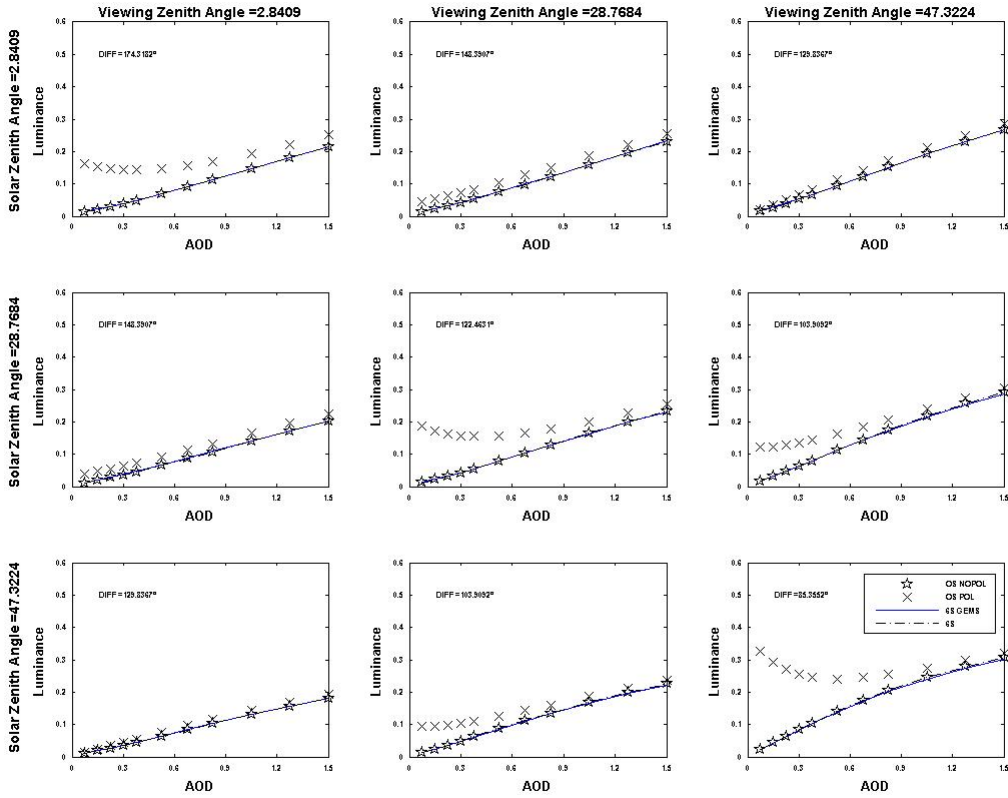


Figure B-34: Same as figure B-33 but for fine mode model 2 with a mean modal radius of $0.08 \mu\text{m}$, standard deviation of 0.46 and a refractive index of 1.60 .

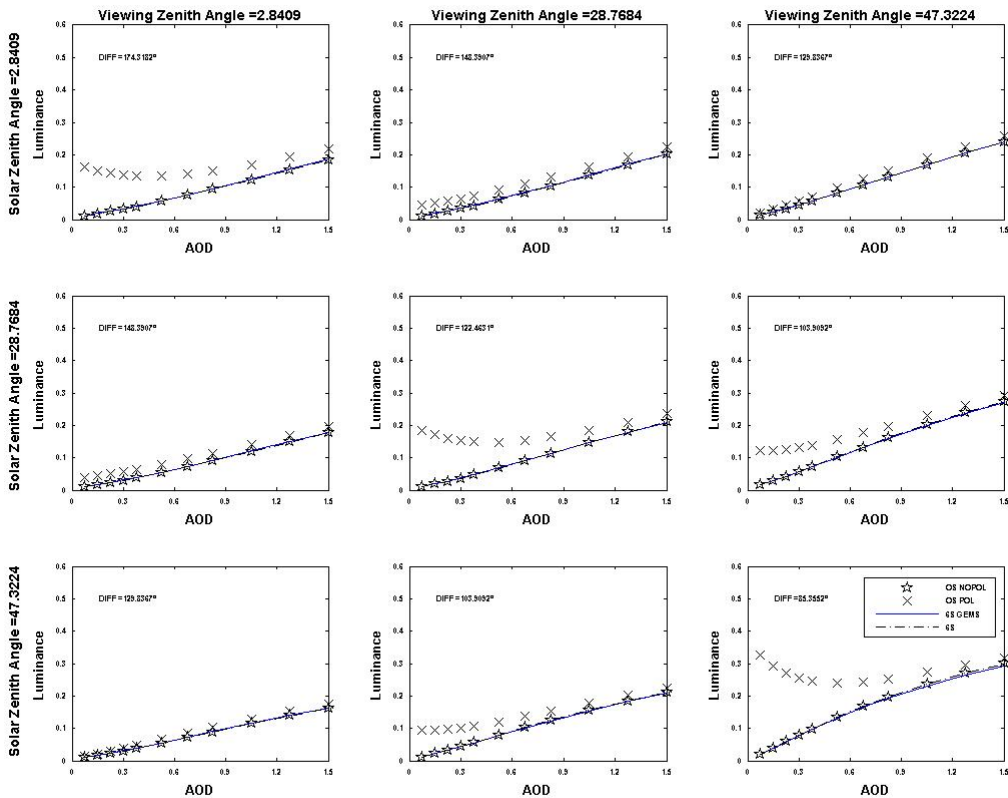


Figure B-35: Same as figure B-33 but for fine mode model 3 with a mean modal radius of $0.1 \mu\text{m}$, standard deviation of 0.46 and a refractive index of 1.60 .

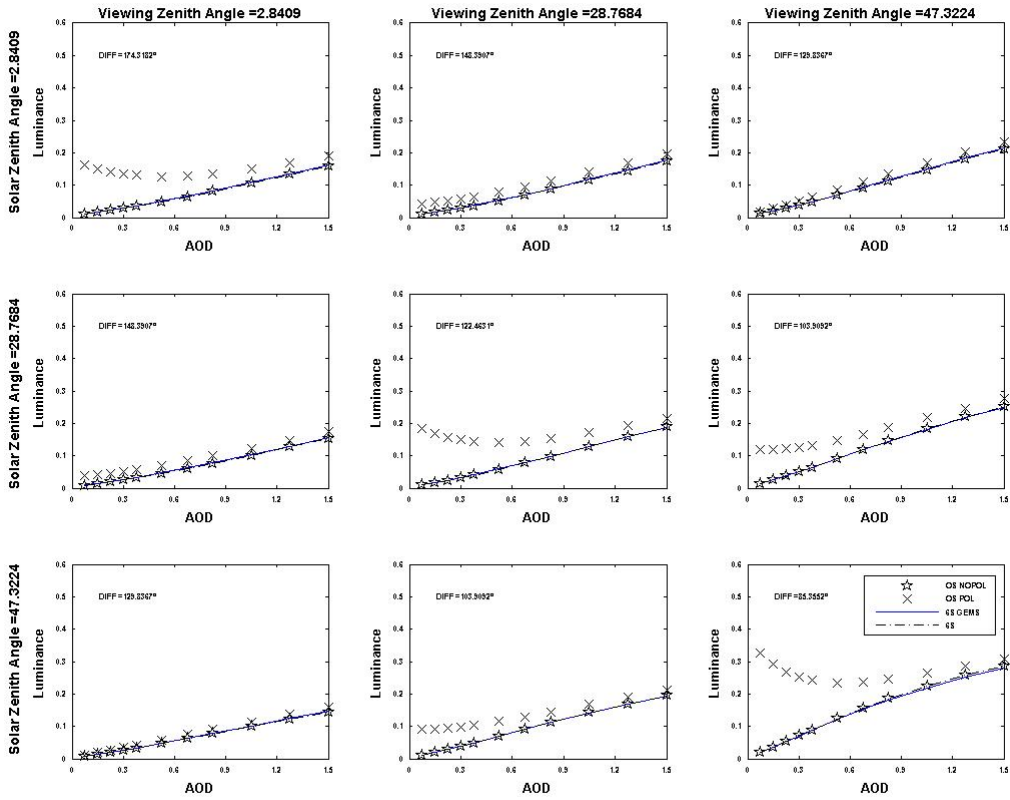


Figure B-36: Same as figure B-33 but for fine mode model 4 with a mean modal radius of 0.13 μm , standard deviation of 0.46 and a refractive index of 1.60.

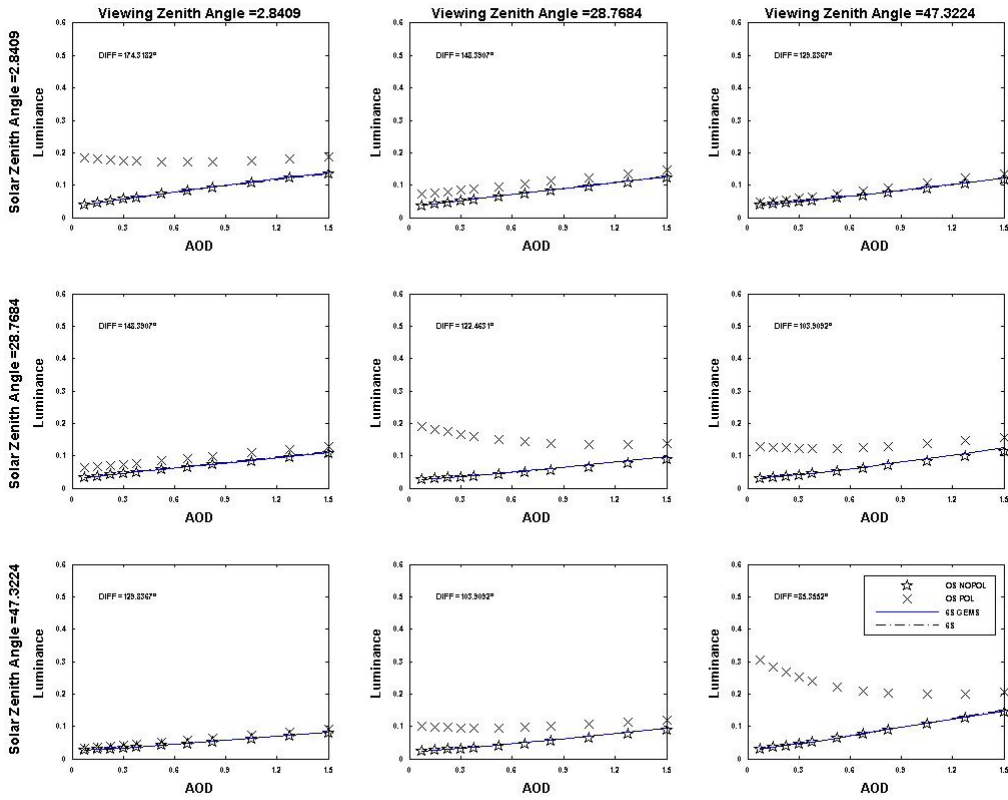


Figure B-37: Radiance according to 6S (black discontinuous), 6S GEMS (blue), OS (stars) and OS without polarization and glitter (black cross) for different solar and viewing zenithal angles. The results correspond to a wavelength of 565 nm, a difference in azimuthal angle of 180°. The aerosol model corresponds to the coarse mode with a mean modal radius of 0.75 μm , standard deviation of 0.7 and a refractive index of 1.33.

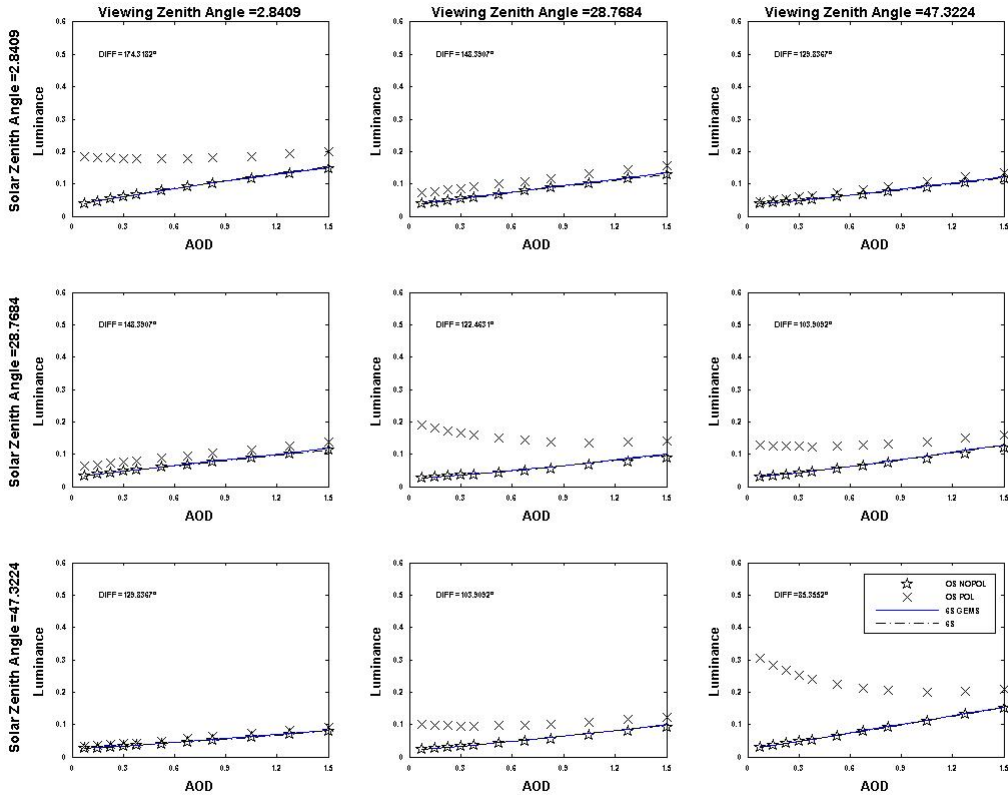


Figure B-38: Same as figure B-37 but for a refractive index of 1.35.

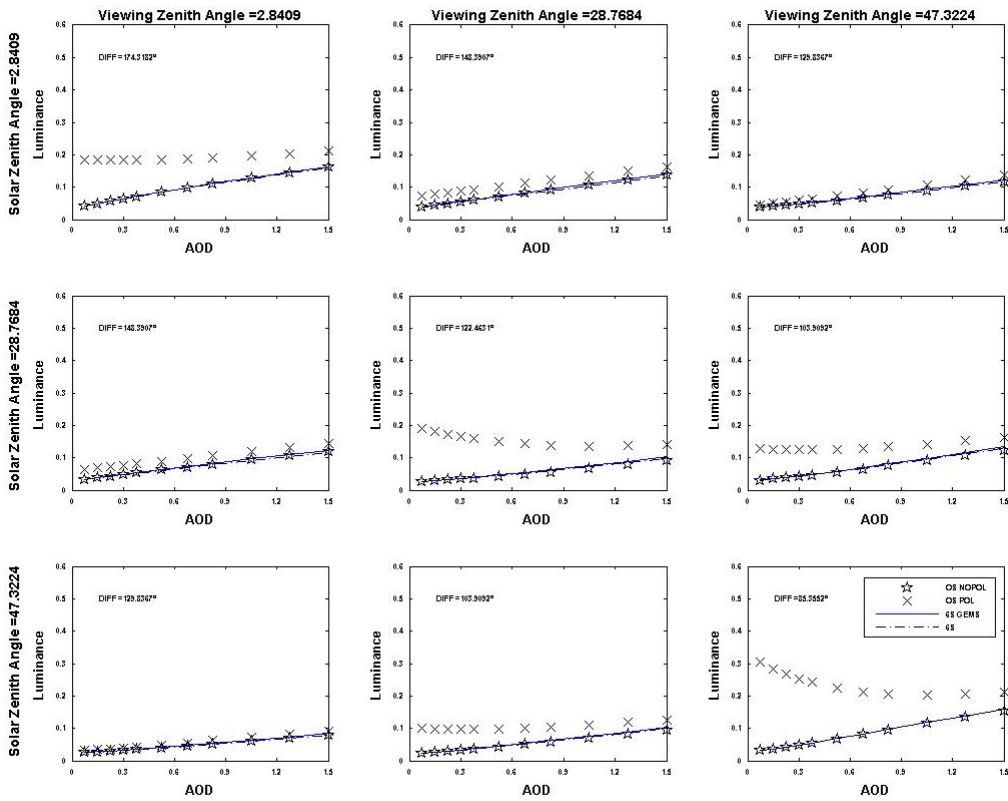


Figure B-39: Same as figure B-37 but for a refractive index of 1.37.

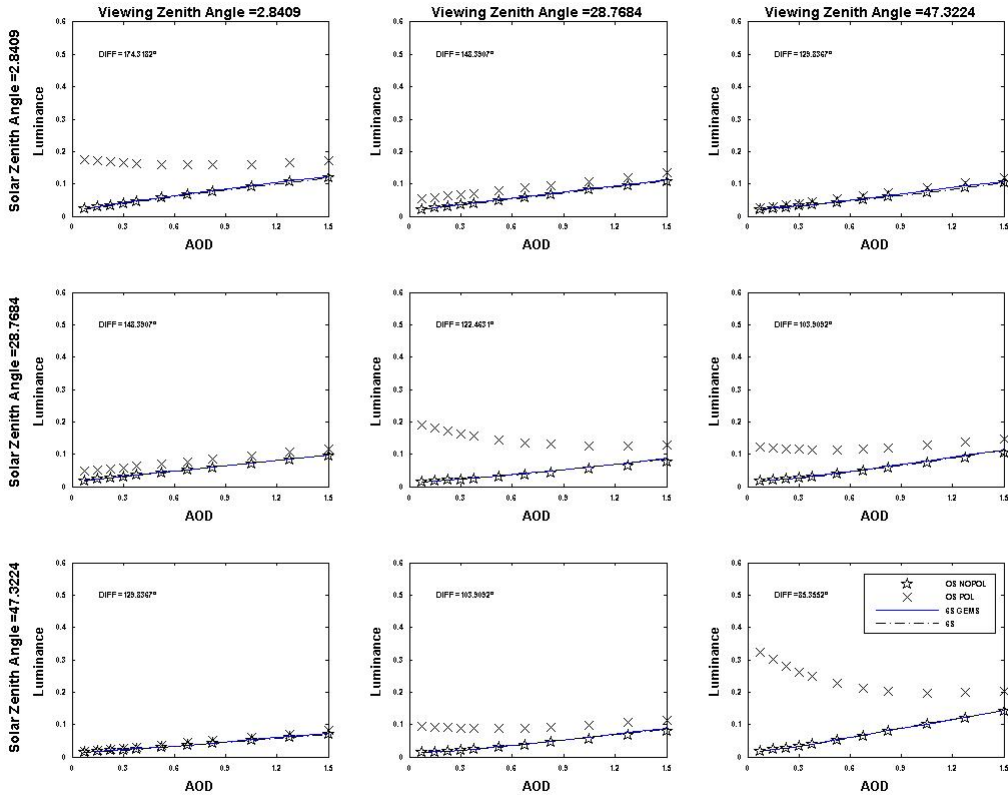


Figure B-40: Radiance according to 6S (black discontinuous), 6S GEMS (blue), OS (stars) and OS without polarization and glitter (black cross) for different solar and viewing zenithal angles. The results correspond to a wavelength of 670 nm, a difference in azimuthal angle of 180°. The aerosol model corresponds to the coarse mode with a mean modal radius of 0.75 μm , standard deviation of 0.7 and a refractive index of 1.33.

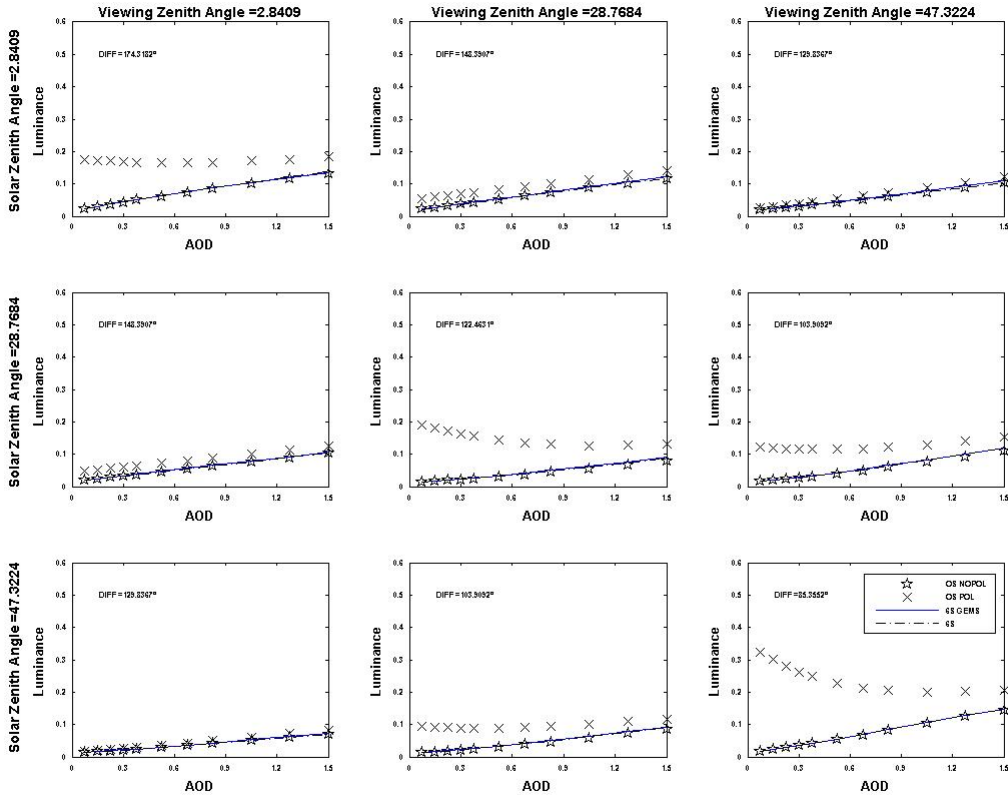


Figure B-41: Same as figure B-40 but for a refractive index of 1.35.

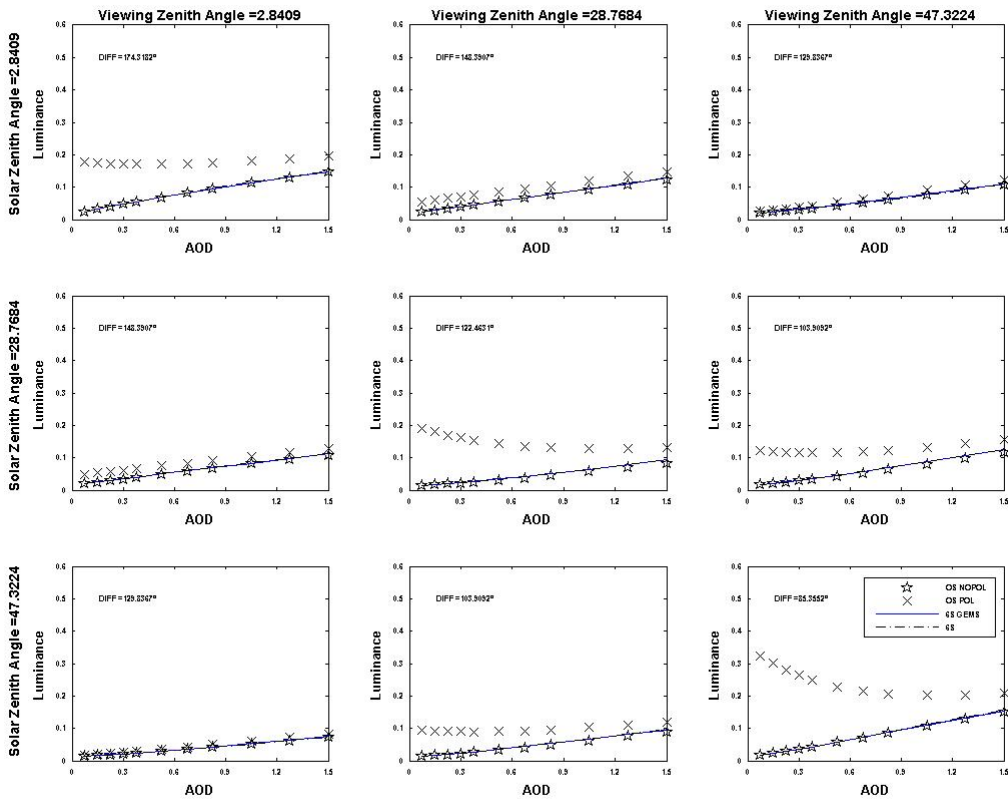


Figure B-42: Same as figure B-40 but for a refractive index of 1.37.

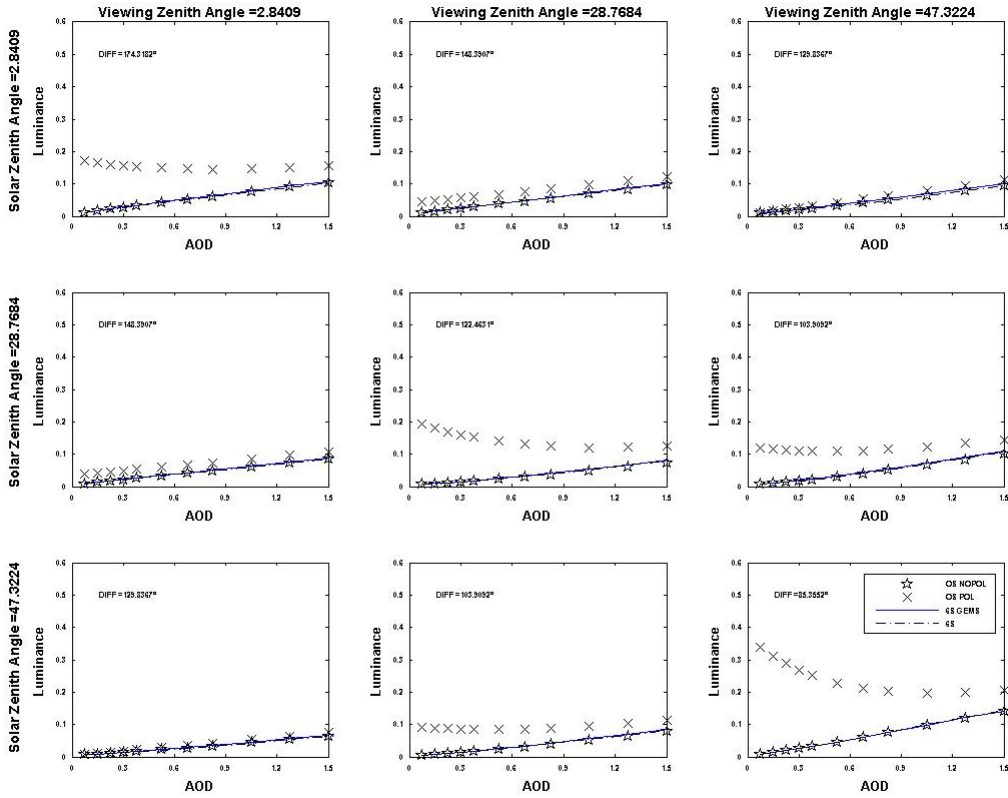


Figure B-43: Radiance according to 6S (black discontinuous), 6S GEMS (blue), OS (stars) and OS without polarization and glitter (black cross) for different solar and viewing zenithal angles. The results correspond to a wavelength of 865 nm, a difference in azimuthal angle of 180°. The aerosol model corresponds to the coarse mode with a mean modal radius of 0.75 μm , standard deviation of 0.7 and a refractive index of 1.33.

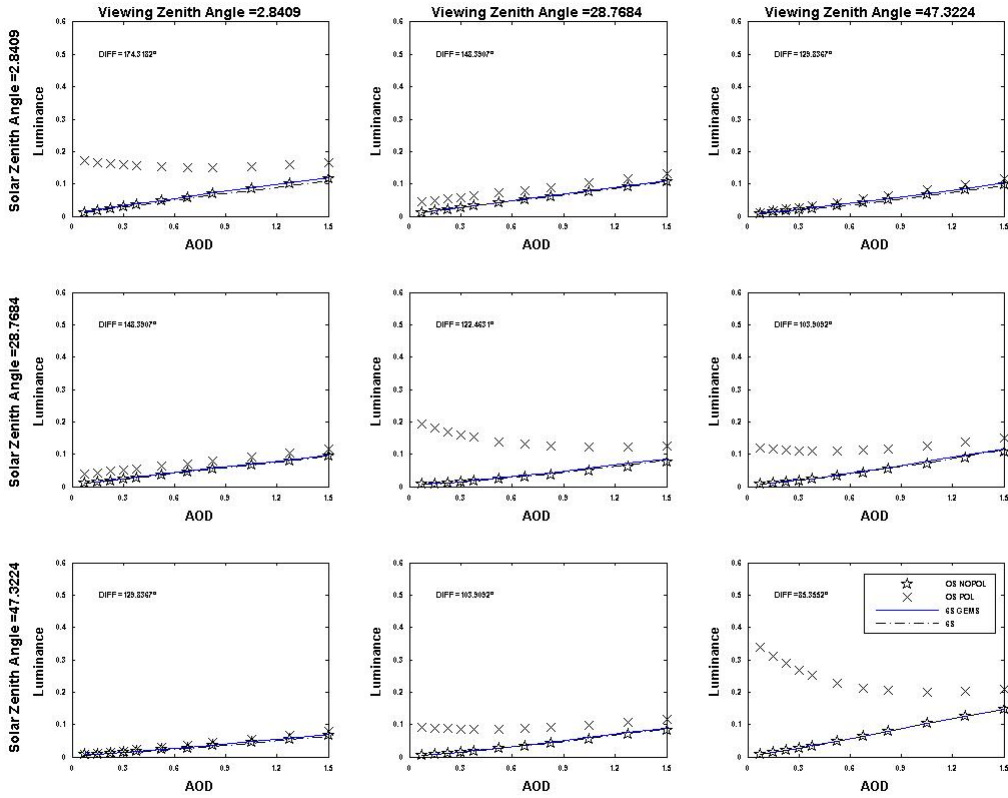


Figure B-44: Same as figure B-43 but for a refractive index of 1.35.

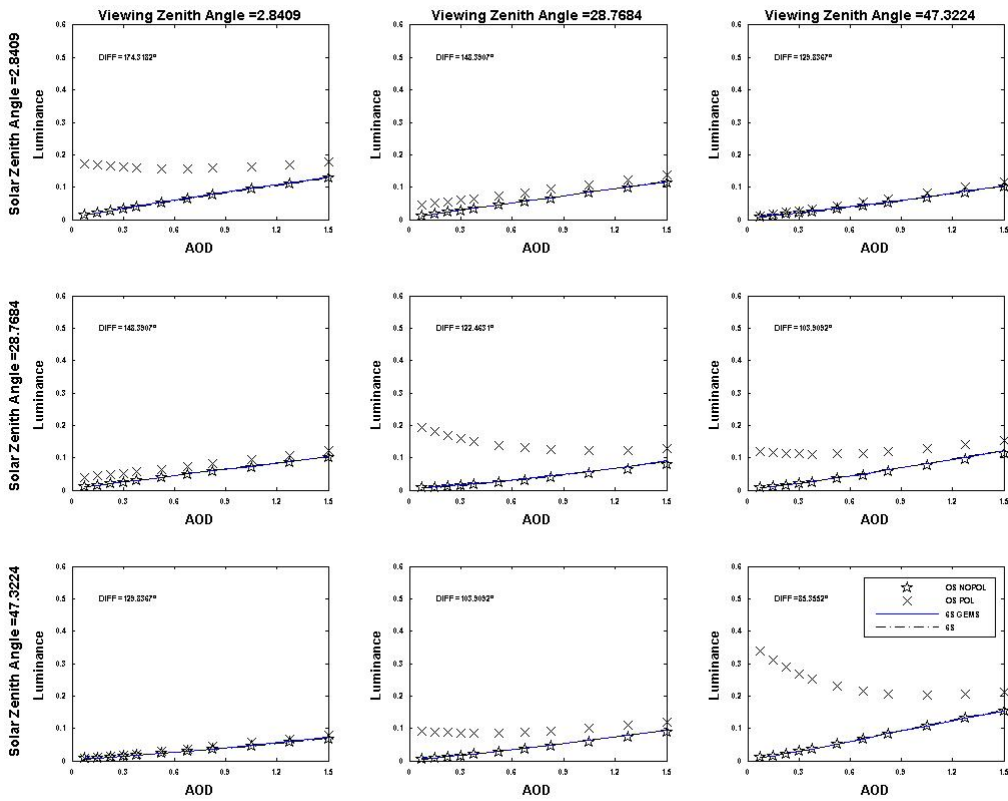


Figure B-45: Same as figure B-43 but for a refractive index of 1.37.